

OPTIMIZATION OF INFILL WELLS IN HETEROGENOUS RESERVOIRS USING A GENETIC ALGORITHM

A Thesis Presented to the Department of
Petroleum Engineering

African University of Science and Technology



In Partial Fulfilment of the Requirements for the Degree of

MASTER of Science in Petroleum Engineering

By

Olayiwola Teslim Olakunle

Abuja, Nigeria

February, 2018.

CERTIFICATION

This is to certify that the thesis titled “OPTIMIZATION OF INFILL WELLS IN HETEROGENOUS RESERVOIRS USING A GENETIC ALGORITHM” submitted to the school of postgraduate studies, African University of Science and Technology (AUST), Abuja, Nigeria for the award of the Master’s degree is a record of original research carried out by Olayiwola Teslim Olakunle in the Department of Petroleum Engineering.

OPTIMIZATION OF INFILL WELLS IN HETEROGENOUS RESERVOIRS USING
A GENETIC ALGORITHM

By

Olayiwola Teslim Olakunle

A THESIS APPROVED BY THE PETROLEUM ENGINEERING DEPARTMENT

RECOMMENDED:

Dr. Akeem Olatunde Arinkoola

Professor David Ogbe

Head, Department of Petroleum Engineering

APPROVED:

Chief Academic Officer

Date

© 2017

Olayiwola Teslim Olakunle

ALL RIGHTS RESERVED

ABSTRACT

Optimal positioning of wells has always been the priority of most reservoir engineers in the face of the dwindling global price of crude oil. As it is always the objective to maximize recoverable reserves over the years, much research has been carried out in order to determine the techniques appropriate for estimating the optimal number and location of wells needed to improve the recovery from a given field.

In this research, well placement optimization in a highly heterogeneous reservoir involving an executable space-filling design and genetic algorithm workflow was developed for improved investment return. The desired objective function was derived using a surrogate-based modelling approach. The objective of this study is to determine and compare the performance of different surrogate modes. The specific objective is the application of the appropriate surrogates in determining the optimal location and completion properties of horizontal wells using space-filling design and genetic algorithms in a complex multidisciplinary optimization problem. This approach was implemented using MATLAB[®] and Schlumberger Eclipse[®] 100. More specifically, surrogates, such as polynomial-based (quadratic, polynomial and multiplicative), geometric-based (kriging and radial basis function) and the integer-based optimizations were modelled as a function of completion properties of a horizontal well using the developed surrogates.

After the numerical simulations, the most economical values of the NPV were estimated. It was observed that the NPV increases as the number of infill wells increases but attains a constant value at optimal value. In addition, the geometric-based models are an effective tool useful in developing surrogate-based rather than polynomial-based models. The results also demonstrate that this method can significantly accelerate the speed of well placement optimization and can help achieve a significant increase in investment return of an actual field if implemented as demonstrated in this case study.

DEDICATION

This thesis is dedicated to God Almighty for the love and infinite mercy bestowed on me throughout the journey.

ACKNOWLEDGEMENTS

First and foremost, I would like to thank God Almighty for His guidance and His protection throughout the period of undertaking this work. The ideas He gave me from time to time when I had challenges were indeed helpful.

Secondly, I express my gratitude to Dr. Akeem Arinkoola for his supervision of this work. Your effort and time spent on this thesis has gone a long way to add quality to it. My sincere appreciation goes to the Head of the Department of Petroleum Engineering, Professor Emeritus David Ogbe for his constructive criticism of this research and for his unrivalled contribution to my personal development. I will forever be indebted, as your scholarly advice has been nothing but a blessing to us all. I also want to thank Schlumberger for donating the Eclipse® reservoir simulator software used for this research.

Thirdly, I would like to express my appreciation for my family especially my dad, mom and siblings for their financial and emotional support throughout the period of this research.

Fourthly, my appreciation goes to my classmates who accepted my excesses throughout our stay in AUST. May our days be plentiful and joyful. See you guys at the top!

Finally, I thank the AUST community and those who contributed to the success of this work either directly or indirectly. Gracias!

TABLE OF CONTENTS

CERTIFICATION.....	ii
ABSTRACT.....	v
DEDICATION.....	vi
ACKNOWLEDGEMENTS.....	vii
TABLE OF CONTENTS.....	viii
LIST OF TABLES.....	xi
LIST OF FIGURES.....	xiv
CHAPTER ONE: INTRODUCTION.....	1
1.1 Background to Study.....	1
1.2 Problem Statement.....	2
1.3 Aim and Objectives.....	3
1.3.1 Aim.....	3
1.3.2 Objectives.....	3
1.4 Scope of Study.....	3
CHAPTER TWO: LITERATURE REVIEW.....	4
2.1 Well Placement Techniques.....	4
2.2 Why Optimize Well-Placement Technique.....	5
2.3 Well-Placement Optimization Algorithm.....	6
2.3.1 Gradient-based method.....	6
2.3.2 Gradient-free Algorithm.....	7
2.4 Surrogate Model.....	11
2.4.1 Polynomial and Quadratic Models.....	13
2.4.2 Kriging Model.....	14
2.4.3 Radial Basis Function (RBF).....	14
2.5 Review of Related Works.....	15
CHAPTER THREE: METHODOLOGY.....	18

3.1	Reservoir Model Description	18
3.2	Determination of Initial Infill Well Location.....	22
3.3	Well Rate Allocation Using Water Cut and Oil Cumulative Production.....	22
3.4	Determination of the Optimum Number of Wells	24
3.5	Surrogate Model Development.....	25
3.5.1	Quadratic Approach.....	28
3.5.2	Polynomial Approach.....	28
3.5.3	Multiplicative Approach.....	29
3.5.4	Kriging-based approach.....	29
3.5.5	Radial Basis Function (RBF) Model.....	30
3.5.6	Model Selection	31
3.6	Optimization	31
CHAPTER FOUR: RESULTS AND DISCUSSIONS		34
4.1	Rate Allocation	34
4.1.1	Analysis of Wells 1, 2, 3 and 4.....	34
4.1.2	Analysis of Wells 5, 6, 7 and 8.....	37
4.1.3	Analysis of Wells 9, 10, 11 and 12.....	39
4.1.4	Analysis of Wells 13, 14 and 15.....	42
4.2	Well Placement Initialization and Maximization.....	44
4.3	Surrogate Model.....	46
4.3.1	Well 1.....	47
4.3.2	Well 2.....	49
4.3.3	Well 3.....	51
4.3.4	Well 4.....	52
4.3.5	Well 5.....	54
4.3.6	Well 6.....	55
4.3.7	Well 7.....	57

4.3.8	Well 8.....	58
4.3.9	Well 9.....	60
4.3.10	Well 10	61
4.3.11	Well 11	63
4.4	Optimization	65
CHAPTER FIVE: CONCLUSIONS AND RECOMMENDATIONS		68
5.1	Conclusions.....	68
5.2	Recommendations	69
REFERENCES.....		70

LIST OF FIGURES

Figure 2.1: Genetic algorithm fundamental principle	8
Figure 2.2: Flowchart for integrated framework of genetic algorithm.....	10
Figure 2.3: Flowchart for integrated framework of PSO algorithm.....	11
Figure 2.4: Frameworks of building surrogate models (modified from Zhong-Hua and Zhang (2012)).	13
Figure 2.5: Different forms of surrogate models	13
Figure 3.1: Framework for optimization work via surrogate-based models	18
Figure 3.2: Reservoir porosity distribution	19
Figure 3.3: Horizontal permeability distribution within the reservoir	19
Figure 3.4: Vertical permeability distribution within the reservoir.....	20
Figure 3.5: Oil and water relative permeability distribution	20
Figure: 3.6 Oil and water relative permeability distribution	21
Figure 3.7: Variation of oil formation volume factor	21
Figure 3.8: Variation of solution gas/oil ratio with pressure	21
Figure 3.8: Frameworks for generating initial wells' location	27
Figure 3.9: Horizontal well direction coding.....	28
Figure 4.1: Crude oil production rate of Wells 1, 2, 3 and 4 for all cases	35
Figure 4.2: Cumulative oil production profile of Wells 1, 2, 3 and 4 for all cases.....	35
Figure 4.3: Bottomhole flowing pressure profile of Wells 1, 2, 3 and 4 for all cases.	36
Figure 4.4: Well water cut profile of Wells 1, 2, 3 and 4 for all cases	36
Figure 4.6: Cumulative oil production profile of Wells 5, 6, 7 and 8 for all cases.....	38
Figure 4.7: Bottomhole flowing pressure profile of Wells 5, 6, 7 and 8 for all cases.	38
Figure 4.8: Well water cut profile of Wells 5, 6, 7 and 8 for all cases	39
Figure 4.9: Crude oil production rate of Wells 9, 10, 11 and 12 for all cases	40
Figure 4.10: Cumulative oil production profile of Wells 9, 10, 11 and 12 for all cases	40
Figure 4.11: Bottomhole flowing pressure profile of Wells 9, 10, 11 and 12 for all cases.....	41
Figure 4.12: Well water cut profile of Wells 9, 10, 11 and 12 for all cases	41
Figure 4.13: Crude oil production rate of Wells 13, 14 and 15 for all cases	42
Figure 4.14: Cumulative oil production profile of Wells 13, 14 and 15 for all cases..	43

Figure 4.15: Bottomhole flowing pressure profile of Wells 13, 14 and 15 for all cases	43
Figure 4.16: Well water cut profile of Wells 13, 14 and 15 for all cases	44
Figure 4.17: Recommended crude oil field production profile	45
Figure 4.18: Results of simulation-based optimization using TPLHD design	45
Figure 4.19: Wells' initial location based on TPLHD.....	46
Figure 4.20: Optimum wells' number and locations.....	46
Figure 4.21a: Fitting results of surrogate models for Well 1 with selective initial points	48
Figure 4.21b: Prediction results of surrogate models for Well 1 with selective initial points.....	48
Figure 4.22a: Fitting results of surrogate models for Well 2 with selective initial points.....	50
Figure 4.22b: Prediction results of surrogate models for Well 2 with selective initial points.....	50
Figure 4.23a: Fitting results of surrogate models for Well 3 with selective initial points	51
Figure 4.23b: Prediction results of surrogate models for Well 3 with selective initial points.....	52
Figure 4.24a: Fitting results of surrogate models for Well 4 with selective initial points	53
Figure 4.24b: Prediction results of surrogate models for Well 4 with selective initial points.....	53
Figure 4.25a: Fitting results of surrogate models for Well 5 with selective initial points	54
Figure 4.25b: Prediction results of surrogate models for Well 5 with selective initial points.....	55
Figure 4.26a: Fitting results of surrogate models for Well 6 with selective initial points	56
Figure 4.26b: Prediction results of surrogate models for Well 6 with selective initial points.....	56
Figure 4.27a: Fitting results of surrogate models for Well 7 with selective initial points	57

Figure 4.27b: Prediction results of surrogate models for Well 7 with selective initial points.....	58
Figure 4.28a: Fitting results of surrogate models for Well 8 with selective initial points	59
Figure 4.28b: Prediction results of surrogate models for Well 8 with selective initial points.....	59
Figure 4.29a: Fitting results of surrogate models for Well 9 with selective initial points	60
Figure 4.29b: Prediction results of surrogate models for Well 9 with selective initial points.....	61
Figure 4.30a: Fitting results of surrogate models for Well 10 with selective initial points.....	62
Figure 4.30b: Prediction results of surrogate models for Well 10 with selective initial points.....	62
Figure 4.31a: Fitting results of surrogate models for Well 11 with selective initial points.....	64
Figure 4.31b: Prediction results of surrogate models for Well 11 with selective initial points.....	64
Figure 4.32: Field oil production rate of the two scenarios	66
Figure 4.33: Field cumulative oil production of the two scenarios	67
Figure 4.34: Comparison of investment cash flow of the two scenarios	67

LIST OF TABLES

Table 3.1: Oil production rate (ORAT) of each horizontal well as used in Cases 2 and 3	24
Table 3.2: Interpretation of well direction coding	26
Table 3.3: Performance indices for model evaluation (Arinkoola & Ogbe, 2015)	32
Table 3.4: Selected genetic algorithm parameters	33
Table 3.5: Selected particle swarm optimization parameters	33
Table 4.1: Summary of the performance indices of surrogate models for Well 1	48
Table 4.2: Summary of the performance indices of surrogate models for Well 2	50
Table 4.3: Summary of the performance indices of surrogate models for Well 3	52
Table 4.4: Summary of the performance indices of surrogate models for Well 4	53
Table 4.5: Summary of the performance indices of surrogate models for Well 5	55
Table 4.6: Summary of the performance indices of surrogate models for Well 6	56
Table 4.7: Summary of the performance indices of surrogate models for Well 7	58
Table 4.8: Summary of the performance indices of surrogate models for Well 8	59
Table 4.9: Summary of the performance indices of surrogate models for Well 9	61
Table 4.10: Summary of the performance indices of surrogate models for Well 10	63
Table 4.11: Summary of the performance indices of surrogate models for Well 11	65

CHAPTER ONE: INTRODUCTION

1.1 Background to Study

Petroleum engineers are often saddled with the responsibility of increasing the amount of recoverable oil or gas obtainable from a given field in order to maximize production and increase profit. In order for petroleum engineers to achieve this, they are faced with the difficulties arising from the heterogeneous nature of the subsurface formation and the uncertainty associated with the estimation of reservoir rock and fluid properties. Because of the aforementioned fact, it has always been described that the field of petroleum engineering is more an art than it is engineering.

In order to achieve maximum recovery in the face of the recent dwindling global price of crude oil, optimal positioning of wells is usually the priority of most reservoir engineers. As it is the objective of reservoir engineers to maximize recovery, there are three production phases, namely, primary, secondary and tertiary production. Primary energy involves the reservoir using its own energy for production. Secondary energy involves using water or gas injection to maintain the reservoir pressure at a favourable level; while tertiary involves other processes such as polymer flooding, CO₂ injection, etc. (Craft & Hawkins, 1959).

By using the conventional method of subsurface reservoir management, the recovery of the original oil initially in place (OOIP) is typically not more than a mere 10% during production using the reservoir energy, but its recovery could be improved considerably using some of the secondary and tertiary recovery methods (DOE, 2008). One of the improved recovery methods is infill drilling which involves drilling new wells into the reservoir so as to increase the oil and/or gas production rate (Salmachi et al., 2013). These wells are drilled in order to shorten the production time, which will increase its net present value in the face of unchanged ultimate recovery. Determining the optimal location and number of infill wells is a crucial phase in infill drilling because it will be a waste of time if the engineer fails to get it right. Of all the positive attributes of infill drilling, the most important is its betterment of area sweep efficiency (Salmachi et al., 2013).

Over the years, much research has been carried out in order to determine the optimal number and location of wells needed to considerably improve the recovery from a given field. The different types of optimization algorithms proposed by different researchers can be grouped into two types, namely, gradient-based and stochastic-based (Sayyafzadeh, 2013). Most of the recently proposed algorithms fall into the stochastic-based category because of their computation efficiency. In this research, the various advantages provided by the genetic algorithm were explored. This was because it has been confirmed to be computationally efficient when determining the number and location of wells needed to improve reserve recovery.

The genetic algorithm is an optimization technique based on the principle of natural selection and genetics proposed by Darwin. The genetic algorithm uses the principle of survival of the fittest (Alexandre, 2009) and proposes a population choosing parameters from a specified range, computing the outcomes and combining the best to form better individuals (Jefferys, 1993). Its first application to optimize a problem was carried out by Holland in 1975 (Holland, 1975). Genetic algorithm is good for nonlinear and discontinuous problems for which classic optimization problems have limited application (Jefferys, 1993).

To perform an optimization problem, it is very important to define the objective function, which in this research, is a maximization problem. Since the optimization problem is an economic one which can either be to maximize cumulative crude oil produced or net present value calculated from revenue and operating cost, that is, CAPEX and OPEX. Possible locations, the number of infill wells, and other parameters modelling the geological and depositional structure of the field are the variables put into the optimization algorithm.

1.2 Problem Statement

Infill well placement operation is a herculean task. It involves accessing a number of possible locations in the face of geological uncertainties. These uncertainties can result in over prediction or under prediction of the optimal number of infill wells. A variety of research has been carried out on how to maximize crude oil production from an unchanged reserve. They have proposed various methods to achieve this, among these is the drilling of infill wells and their placement.

In order to maximize the well placement operation, various optimization techniques were proposed. In all these, GA is adjudged more effective in optimizing problems, especially those with nonlinear variables.

As can be observed in results from previous work, well placement was viewed as a non-intuitive problem (Yeten, 2003). This motivated other researchers to design a generalized optimization algorithm for the determination of the optimal number and location of infill wells. It is also important to stress that the desire to use GA in well placement optimization stems from its advantages observed in previous applications for field development as well as its ability to perform successfully in complex search operations.

1.3 Aim and Objectives

1.3.1 Aim

The aim of this study is to determine optimal location and configuration of infill wells in a heterogeneous reservoir using a genetic algorithm

1.3.2 Objectives

The following are the objectives of the aforementioned aim:

- i. Building a synthetic model with heterogeneity;
- ii. Development of a generic framework for infill well placement optimization;
- iii. Determination of the initial infill well locations;
- iv. Development of a proxy model with NPV objective function;
- v. Optimization using a genetic algorithm.

1.4 Scope of Study

This research is limited to the optimization of infill wells in heterogeneous reservoirs using a genetic algorithm. The numerical simulation was limited to the use of the Schlumberger Eclipse[®] black oil simulator. The GA was implemented using MATLAB[®].

CHAPTER TWO: LITERATURE REVIEW

2.1 Well Placement Techniques

Well placement is a comprehensive planned action used in positioning wells in order to maximize productivity or injectivity (Griffith, 2009). The basic aim of any drilling operation is to locate correctly the hydrocarbon rich zone. Because of this, the well orientation becomes a critical factor dependent on the nature of the subsurface formation, which is obtained from the seismic well log analysis, well testing and production data. Despite these readily available parameters, most well-placement techniques have suffered because of a high degree of subsurface heterogeneity present within a small resolution. Most traditional well-placement techniques can be classified under the following categories (Griffith, 2009):

A. Model, compare and update (MCU)

This is a method that uses log responses to build a geological model representative of the formation under study, depicting the subsurface as well as the well trajectory. In this type of well-placement technique, the parameters used were obtained from responses such as gamma ray, resistivity, density and neutron responses obtained in real time using measurements while drilling (MWD) but transmitted using logging while drilling (LWD).

B. Real-time dip determination

Here, the limitation inherent with the use of the MCU technique was solved by the introduction of azimuthal measurements, which have the ability to differentiate between boundaries near the well above from the one approaching from below, namely, well direction savvy. This technique uses data obtained from wellbore sides and extrapolates to calculate other parameters far from the wellbore. This technique assumes that the formation dip varies insignificantly.

C. Remote detection of boundaries

Azimuthal data improves well-placement operations by aiding the accurate determination of direction of contact to the borehole but suffers from a lack of investigation depth.

Remote detection techniques use azimuthal data coupled with seismic data to account for the limitation associated with the use of azimuthal measurements only. Also, this well placement technique uses an inversion process to convert raw directional and attenuation measurements to a layered geological model where the distance and direction of the formation's resistivity changes are obtainable.

2.2 Why Optimize Well-Placement Technique

In well-placement operations, the following parameters are critical to effectively describing the well position:

- A. True vertical depth;
- B. Displacement;
- C. Azimuth;
- D. Inclination.

Due to the high degree of heterogeneity present within the subsurface formation, the determination of well placement has suffered from either overestimation or underestimation. Because of this, optimization of well-placement techniques is very important. According to Wang et al. (2016), and Dossary and Nasrabadi (2016), well-placement optimization technique is described as a complex, nonlinear and multidimensional operation.

In addition, due to the falling global price of crude oil and the increase in demand, it is important to determine correctly the position and orientation of the well. Below are some of the reasons for well-placement optimization (Dossary & Nasrabadi, 2016; Onwunalu & Durlofsky, 2009; Afshari et al., 2014; Chen et al., 2017):

- A. Correctly determine the well position;
- B. Correctly determine the optimum number of wells needed to effectively drain the reservoir;
- C. Maximize recoverable reserves;
- D. Optimize crude oil and gas production while reducing water production;
- E. Limit the number of wells.

2.3 Well-Placement Optimization Algorithm

Most engineering problems involve the selection of one or more variables that can correctly optimize a given set of objective functions (Iqbal, 2013). This process is termed optimization and has been used extensively in the past 20 years in product design and quality checking, either with the aid of computer simulation or using manual techniques.

Equation 1 gives the general configuration of the optimization technique

$$\begin{aligned} & \text{Min / Max } F(X): \text{Objective function} \\ & \text{Subject } \sum_{i=1}^n \lambda_i X > 0: \text{Inequality constraint} \\ & \sum_{j=0}^n \lambda_j X = 0: \text{Equality constraint} \end{aligned}$$

The complexity of each problem increases with number of parameters under study. Mathematical formulation of the problem is expected in the aforementioned equation. In finding the global minimum or maximum, there is generally a trade-off between speed, degree of robustness and likelihood (Reed & Marks II, 1999).

Most well placement optimization algorithms can be classified as either deterministic (evaluation or gradient based) or stochastic (gradient free) (Dossary & Nasrabadi, 2016; Vu et al., 2015).

2.3.1 Gradient-based method

This is a simple method that uses the derivative of its objective function in the determination of the optimal variable(s). Examples include:

- i. steepest descent;
- ii. conjugate gradient descent;
- iii. Newton's method;
- iv. Gauss-Newton method;
- v. Levenberg-Marquardt method;
- vi. quasi-Newton method.

Most gradient-based methods converged to the same value if the same initial estimate was used. Most deterministic methods failed because of their inability to model correctly the nonlinearity and non-continuous nature of oil field variables (Montes et al. 2001).

2.3.2 Gradient-free Algorithm

The absence of derivatives makes the use of the gradient-free optimization algorithm important (Vu et al., 2013). A gradient-free optimization algorithm is a simple but problem-specific optimization algorithm. This algorithm can tolerate a high degree of noise inherent in functions under specific conditions. According to Ciaurri et al. (2013), Hosseini S. & Al Khaled A. (2014) , Guyaguler & Horne (2002) and Ebadat & Karimaghaee (2001), gradient-free algorithm application has been found in oil and gas operations in areas such as history matching, parameter estimation and production optimization.

The efficiency of this optimization algorithm depends on the type of algorithm used (Montes et al. 2001; Vu et al., 2013). Examples of gradient-free algorithms include genetic algorithm (Emerick et al., 2009; Monte et al., 2001; Salmachi et al., 2013), simulated annealing (Bangerth et al., 2006; Beckner & Song, 1995), particle swarm optimization (Onwualu & Durlinsky, 2009), the differential evaluation algorithm (Carosio et al., 2015; Awotunde, 2014), cat swarm optimization algorithm (Chen et al., 2017), artificial bee colony (Xu et al., 2013; Sayyafzadeh et al., 2012), imperialist competitive algorithm (Dossary & Nasrabadi, 2016) and bat-inspired algorithm (Naderi & Khamehchi, 2016).

2.3.2.1 Genetic Algorithm

Genetic algorithm (GA) is one of the most widely used metaheuristic optimization algorithms. GA is an algorithm based on the principle of natural selection as proposed by Darwin's evolutionary theory (Montes et al., 2001). According to Montes et al. (2001), GA was first used by John Holland to model a complex task effectively and he confirmed that GA could overcome shortcomings associated with the use of gradient-based algorithms.

Genetic algorithm has found its application in areas of specialization ranging from the optimization of gas transmission lines (Goldberg 1993), nonconventional well optimization (Yeten et al., 2003; Onwunalu, 2005), reservoir modelling and description (Guerreiro et al., 1997), history matching (Askari Firoozjaee & Khamehchi, 2015), pressure drop prediction (Ebrahimi & Khamehchi, 2015), gas lift design (Rasouli et al., 2015) and others.

The underlining principles inherent in GA are shown in Figure 2.1.

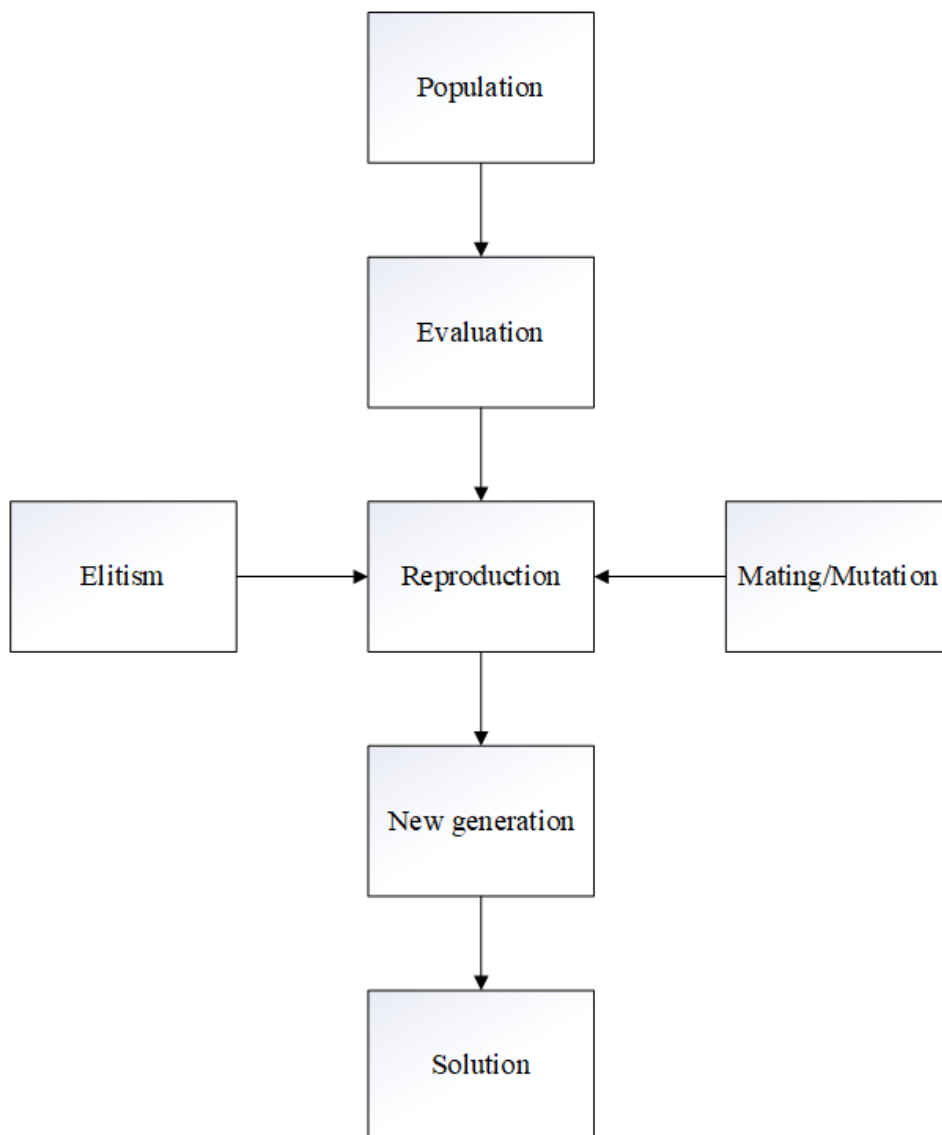


Figure 2.1: Genetic algorithm fundamental principle

Some terms used in GA include:

- i. Population - this refers to a set of possible outcomes of a given problem and is synonymous with human population.
- ii. Chromosomes – this refers to one of the possible outcomes contained in the population and is encoded in either binary or real numbers.
- iii. Gene or Individual – this refers to a potential solution to an optimization problem and also the parameters defining a particular element of a chromosome.
- iv. Genotype – this represents population in the computational space and also refers to the way solutions are codified in computing systems. This can be represented in binary, real values, integers or permutations.
- v. Allele – this refers to the value a gene takes for a particular chromosome.
- vi. Phenotype – this represents population in the real world and refers to the way solutions are codified in the real world.
- vii. Fitness, also known as objective function – this refers to a function which takes the solution as input and returns the suitability of the solution as the output.
- viii. Genetic operators – these are tools used to alter the genetic composition of offspring during reproduction. These include mutation, crossover and selection.
- ix. Seed – this refers to the initial population of an algorithm.
- x. Parents – this refers to two individuals that are genetically fit to undergo reproduction.
- xi. Offspring – this refers to individuals resulting from reproduction.
- xii. Reproduction – this refers to the process controlling how new generations are formed and here, individuals with the best fitness value in the preceding generation as having a higher probability of surviving in the next generation.

Population generation is the first step in a typical GA algorithm where specified variables are codified to form chromosomes. This results in an initial population that can either reproduce automatically or manually (Montes et al., 2001). After this step, the initial population, i.e. the chromosomes, are evaluated by ranking them from best to worst. The good chromosomes are retained and used in the next generation during reproduction while the poor ones are discarded. In the reproduction phase,

three processes, namely, mating, mutation and elitism are used. The differences between the three processes are that, in elitism, some of the parent chromosomes are passed to the new generation while, in mating, two chromosomes are crossed to form new ones, but mutation involves the change in genetic composition of the parent chromosomes. Figure 2.2 shows the description of the integrated framework in GA.

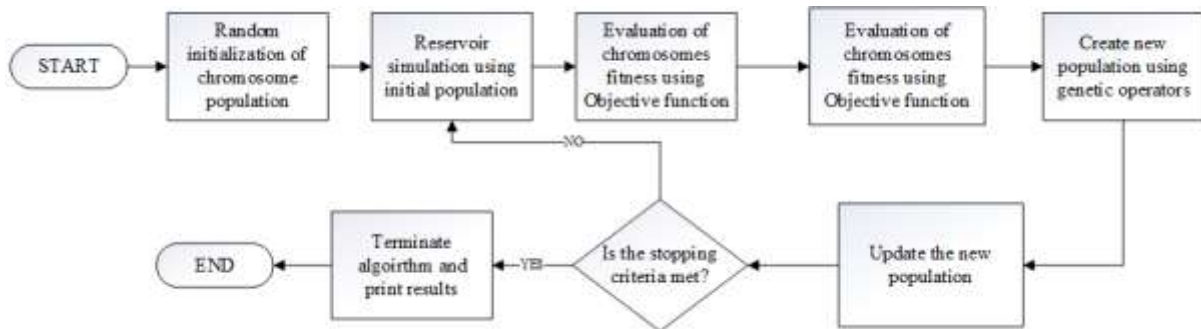


Figure 2.2: Flowchart for integrated framework of genetic algorithm

2.3.2.2 Particle Swarm Optimization

Particle swarm optimization (PSO) is a relatively new algorithm (Davis, 1991; Cleric, 2006; Eberhardt & Kennedy, 1995; Engelbrecht, 2005; Kennedy & Eberhardt, 1995), similar to the genetic algorithm (Davis, 1991) because both algorithms are initialized randomly with a stochastic-based solution (Russell & James, 1995). Its application can be found in solving complex nonlinear problems such as well placement (Onwunalu & Durlofsky, 2011; Naderi & Ehian, 2016), reservoir modelling (Rwechungura et al., 2014) and optimization of field development programme (Isebor et al., 2014). This algorithm was first developed by Kennedy and Eberhardt in 1995 (Eberhardt & Kennedy, 1995).

This algorithm mimics food-finding behaviour, that is, the social interaction of fish and birds while trying to avoid predators by sharing information with fellow species (Onwualu & Durlofsky, 2009). In a typical PSO algorithm, the determination of particle (that is, potential solution) position and velocity is very important. A particle represents a point in space, that is, an individual or one of the possible outcomes, while a swarm refers to the population, that is, a set of all possible outcomes

(Onwualu & Durlinsky, 2009; Eberhardt & Kennedy, 1995; Kennedy & Eberhardt, 1995).

In a particle swarm optimization algorithm, the objective function is to obtain the current location of each particle. Each particle then determines its bearing within the search space by adding its own history and best location, namely, fitness with other members within the population (swarm) randomly. Pbest and gbest are the two solutions each particle within the population hopes to attain (Russell & James, 1995). The pbest is the best solution achieved by the particle in the hyperspace, while the gbest is the best overall value, that is, the global version of the optimizer attained by the particle. In obtaining the optimal solution, the updating of particle velocity and position is done using three stochastically defined parameters, namely, inertia factor, self-confidence and swarm confidence factor (Kennedy & Eberhardt, 1995; Engelbrecht, 2005; Poli et al., 2007; Onwualu, 2010). Figure 2.3 shows the description of the integrated framework involved in PSO.

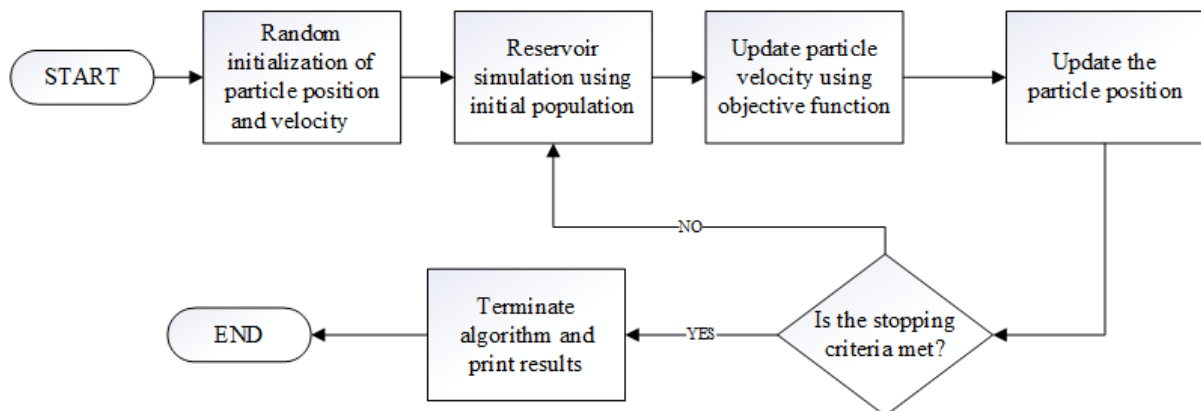


Figure 2.3: Flowchart for integrated framework of PSO algorithm

2.4 Surrogate Model

Surrogate model is a technique used when an output of interest cannot be measured directly with ease. The surrogate model can be either a cost function or a state function (Han & Zhang, 2012) built using data points obtained from random experiments. Surrogate-based models are also known as metamodels, response surface models, approximation models or emulators (Han & Zhang, 2012; Vu et al., 2015).

Most simulation-optimization models usually take hundreds or thousands of times to reach convergence (Johnson & Rodgers, 2001; Wan & Zeng, 1997) and, as such, have been found to be computationally costly (Chen et al., 2017). Due to the aforementioned fact, most simulation-optimization models are being modelled using surrogate-based modelling because it is efficient and computationally cost-effective (Han & Zhang, 2012; Chen et al., 2017). As such, the main purpose of developing a surrogate-based model is to iteratively construct or design a computer model that can correctly model the behaviour of the physical phenomenon under study (Vu et al., 2015; Chen et al., 2017).

The first step in building a surrogate-based model, as shown in Figure 2.4, involves generating initial data points. This can be achieved using design of experiment (DOE) (Giunta et al., 2001). DOE is a technique aimed at maximizing the available information from a limited number of sample points (Giunta et al., 2001). DOE methods include classic types such as full-factorial design, central-composite design, Box-Benken design, D-optimal design and modern DOE types such as Latin hypercube design (LHD), translational propagation Latin hypercube design (TPLHD), orthogonal array and uniform design (Fang et al., 2000; Giunta et al., 2001). Latin hypercube design (LHD) has found its application in various fields such as non-collapsing and space-filling designs because of its better computational efficiency compared to classic DOEs (McKay et al., 1979; Vu et al. 2011). According to Pan et al. (2014) and Viana et al. (2010), TPLHD obtains optimal or near-optimal Latin hypercube design with minimal computational effort and without formal optimization. This research focuses on the use of TPLHD in generating initial points to be used in the development of the surrogate-based model.

Onwunalu (2006) stated that metamodels accelerate the optimization process by accelerating the convergence rate and reduction of iteration numbers, but do not affect the solution-generating characteristics of most metamodeling techniques.

According to Han and Zhang (2012), surrogate-based models can be developed using techniques or methods such as polynomial, quadratic, radial basis function, kriging, multiplicative and artificial neural networks (ANN).

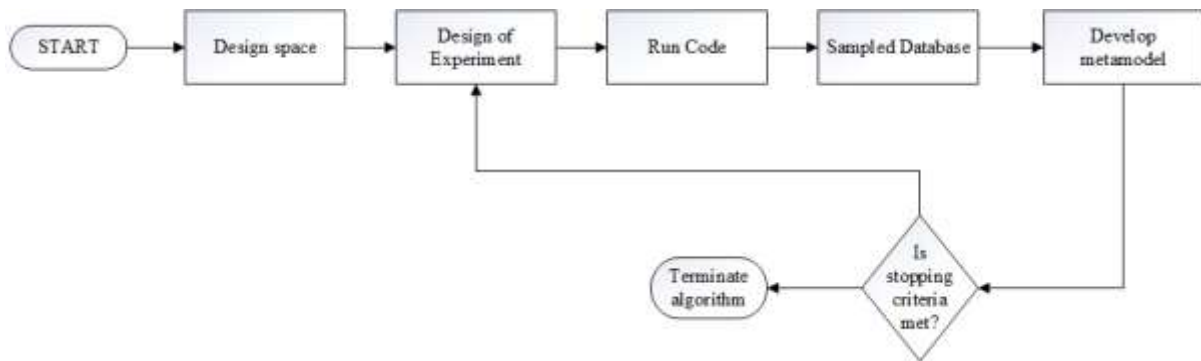


Figure 2.4: Frameworks of building surrogate models (modified from Han and Zhang (2012)).

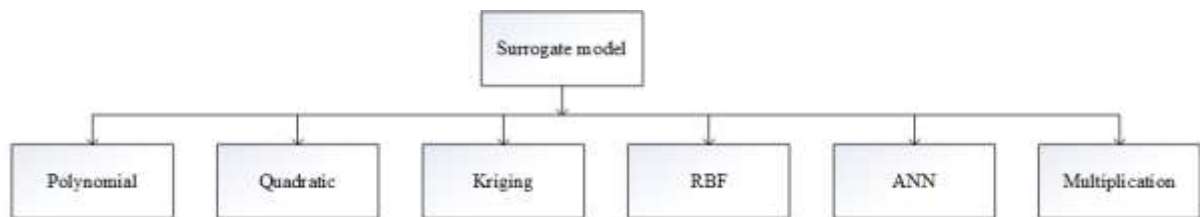


Figure 2.5: Different forms of surrogate models

2.4.1 Polynomial and Quadratic Models

Here, the response surface modelling approach is used to fit the sampled data by using the least squared approximation technique. The quadratic method aids the smoothing out of various degrees of noise present in most measured sample data while polynomial models have the advantage of capturing the noise due to their higher order of nonlinearity. This technique also captures the global trend of the variation (Han & Zhang, 2012). The general form of both the quadratic and polynomial models is given as:

Quadratic model

$$Y = \text{constant} + \text{Coefficient} \times (X_i) + \text{Coefficients} \times \text{interactionterms}(\text{order}2)$$

Polynomial model

$$Y = \text{constant} + \text{Coefficient} \times (X_i) + \text{Coefficient} \times \text{interactnterms}(\geq \text{order}2)$$

2.4.2 Kriging Model

This was first introduced by Krige in 1951. It is an interpolation technique based on geostatistics that approximates the spatial correlation between the sampled points. According to Han and Zhang (2012), the kriging technique has been found to be well suited to modelling the nonlinear function of the higher order. Its application has been found in the optimization of nozzle problems (Simpson et al., 1998), design of experiments (Sacks et al., 1989), mathematical modelling (Jin et al., 2000), prediction of reservoir accumulation outflow (Mohammadi et al., 2012) and optimization of well locations (Guyaguler, 2003). Below is the generalized kriging model:

$$Y(x) = f^T(x)\beta + z(x), x \in IR^m$$

where

$$f(x) = [f_0(x) f_1(x) \dots \dots \dots f_{P-1}(x)]^T$$

$$\beta = [\beta_0 \beta_1 \dots \dots \dots \beta_{P-1}] \in IR^m$$

2.4.3 Radial Basis Function (RBF)

RBF is another metamodeling function where the approximate output of an unknown function $U(x)$ at an untried location x is given linearly by the equation below:

$$U(x) = \sum_{i=1}^m v_i X(x) + N(x)$$

subject to the following constraints

$$y(x^i) = y^i, i = 1, 2, 3 \dots m$$

$$\sum_{i=0}^m v_i = 0$$

where

$X(x)$ = basis function which is a function of geometric distance between the point of interest x^i and untried point x .

$N(x)$ = global trend function

v_i = weight coefficient of variable i .

According to Han and Zhang (2012), and Pan et al. (2014), the commonly used forms of radial basis function include Gaussian, power, spline and Hardy's multi-quadratic and inverse multi-quadratic functions.

RBF has gained a wide range of applications because of its simplicity and accuracy in modelling nonlinearities present in approximation problems (Babu & Surech, 2013; Yao et al., 2014; Vukovic & Milvovic, 2013; Couckuyt et al., 2013). In addition, RBF is a better choice because of its ability to use limited numbers of sampling points in computationally expensive functions (Pan et al., 2014). The use of RBF has been applied to such areas as classification problem (Babu & Surech, 2013), optimization (Yao et al., 2014; Katayama et al., 2013), function approximation (Vukovic & Milvovic, 2013) and modelling of microwave structure (Couckuyt et al., 2013).

2.5 Review of Related Works

Several works have examined the application of various optimization techniques in optimizing well placement. Most applied techniques have yielded favourable results. Of all the optimization algorithms used, evolutionary-based and metaheuristic-based algorithms have proven to be efficient and effective techniques.

Bittencourt et al. (1997) used a hybridized genetic algorithm combined with an integrated economic model and simulation design to determine the optimal location of wells and their configurations. They used ninety-nine decision variables and observed that the forecast outputs would have an improvement of about 6% in profit if implemented.

Montes et al. (2001) applied a non-hybridized genetic algorithm in optimizing vertical wells with the objective function being a technically based cumulative oil production. Here, two synthetic reservoirs were used, and it was found that elitism improved the solution convergence rate optimally. They also concluded that, rather than replacing geological and technical parameters with automated well placement techniques, they should be combined to complement each other.

Kabir et al. (2002) introduced the use of experimental design on modelling uncertainties in geological and engineering parameters. With this approach, both the linear and non-linear impacts were captured. They used a response surface model as the objective model and concluded that geological features have a greater influence on the result than reservoir heterogeneity.

Guyaguler et al. (2000) applied a hybrid binary encoded genetic algorithm optimization technique and, in addition, used the approach used by Bittencourt et al. Kriging and artificial neural networks were used as proxies. Here, the location of four vertical injectors for a water-flooding project was studied and it was concluded that the kriging-based technique was better than that of the artificial neural network for the problem studied.

Yeten (2003) used a genetic algorithm coupled with several helper functions such as an artificial neural network and the hill climber technique to enhance the effectiveness of the algorithm. A proxy model was developed using an artificial neural network and it was found that net present value or cumulative oil production increased by approximately 30 % in each scenario studied. It was concluded that the optimum well type depends on the reservoir type, objective function and degree of uncertainty.

Salmachi et al. (2013) applied a genetic algorithm in a coalbed methane reservoir. Here a simulator was coupled with the algorithm using net present value as the objective function. It was assumed that the dual porosity system, the Langmuir adsorption isotherm hold and the developed framework were validated using a standard 5-spot well placement pattern. They noticed that the quality of the sweet spot is a function of reservoir rock and fluid properties, as well as economic parameters. In addition, coalbed infill well drilling is profitable if and only if the water production is at an economical level as a result of a lower gas price.

Moravvej (2008) used a continuous genetic algorithm rather than the widely used binary coded genetic algorithm in the optimization of well placement. It was concluded that the efficiency of a genetic algorithm search can be increased by introducing a minimum Euclidean distance between wells within the population.

Lyons and Nasrabadi (2015) applied an ensemble Kalman filter and a genetic algorithm on well placement optimization under time-dependent changes. The Kalman filter was used to continuously update the reservoir model in order to account for the uncertainties arising from the drilling of wells at different times as

against the assumption that wells are drilled simultaneously. It was concluded that an ensembled Kalman filter reduces the computational time required for optimization.

Onwunalu and Durlosfky (2010) applied PSO in the determination of the optimal well type and location in order to maximize the net present value. Here, they studied four different cases, namely, optimization of single and multiple realizations of deviated and dual lateral wells. In addition, it was observed that PSO outperforms GA in all scenarios and the advantages of PSO change from case to case.

CHAPTER THREE: METHODOLOGY

To optimize the number and location of wells required to maximize the reserve obtainable from a reservoir, it is customary to build a black box model for simulation. Since most reservoirs are highly heterogeneous, their effective management is difficult due to the high randomness of their properties, such as porosity and permeability. In this study, a numerical reservoir simulator and metamodels were used. Optimizations were carried out using nature-inspired algorithms, which have been found to perform excellently in most of the field applications. An integrated approach that summarizes the aforementioned steps and methods is shown in Figure 3.1.

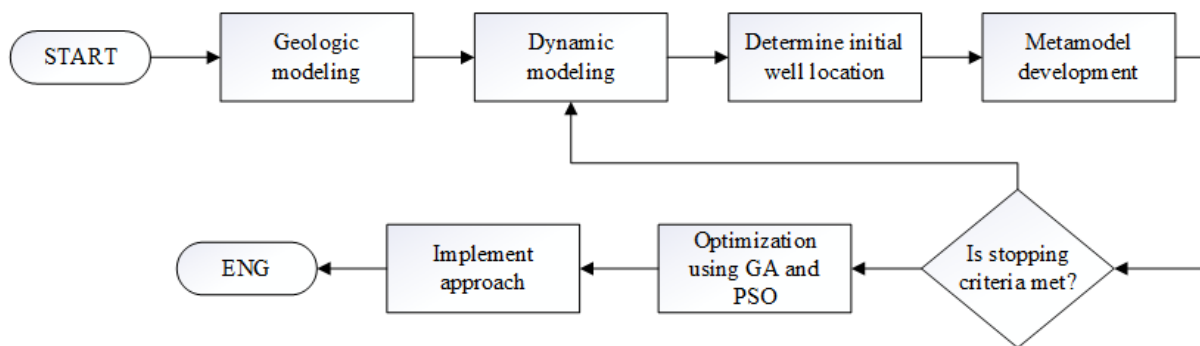


Figure 3.1: Framework for optimization work via surrogate-based models

3.1 Reservoir Model Description

The synthetic model used for the analysis was obtained from the Society of Petroleum Engineers' Comparative Solution Project developed by Killough in 1995. The SPE 9 reservoir model's grid is 24*25*15 with the reservoir tops located at 9800 ft ss. Each X and Y grid block has a dimension of 300 ft and a total of 9000 active blocks. The reservoir grid was based on the conventional rectangular coordinates with no local grid refinement. The reservoir model was partitioned into fifteen layers to adequately capture the heterogeneity inherent within the reservoir. Based on the modification effected on the original reservoir simulation data developed by Killough, the reservoir was assumed initially to contain two vertical wells. The gas oil contact and water oil contact are located at 9876 ft and 9989 ft respectively. The oil, water and gas densities at the surface are given as 44.98 lb/ft³, 63.01 lb/ft³ and 0.0702

lb/ft³ respectively. The porosity and permeability distribution for the reservoir are as shown in Figures 3.2, 3.3 and 3.4. The distribution of the relative permeability of the gas, oil and water at different saturations are shown in Figures 3.5 and 3.6. Figures 3.7 and 3.8 show the distribution of solution gas/oil ratio and oil formation volume factor at varying reservoir pressures.

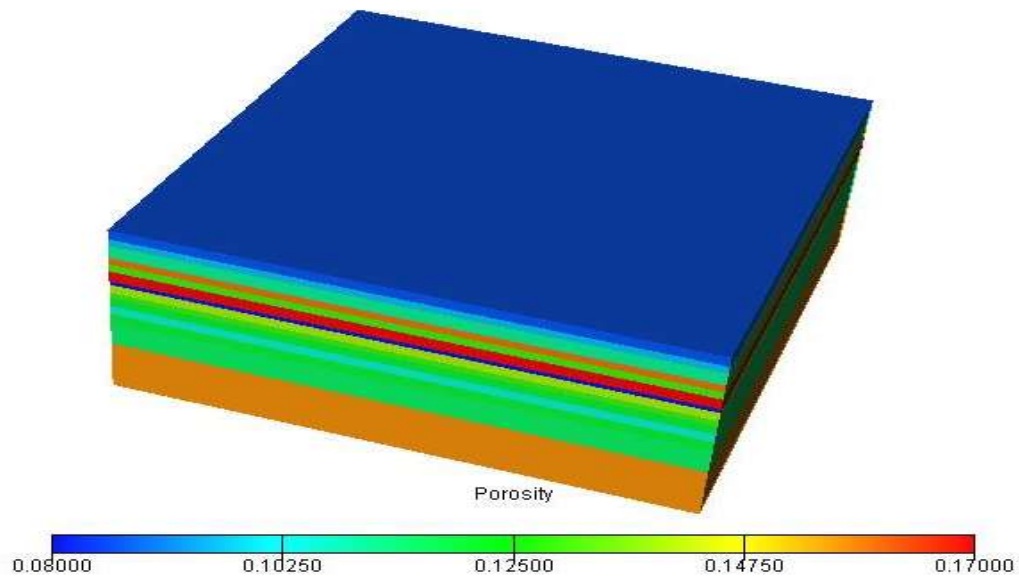


Figure 3.2: Reservoir porosity distribution

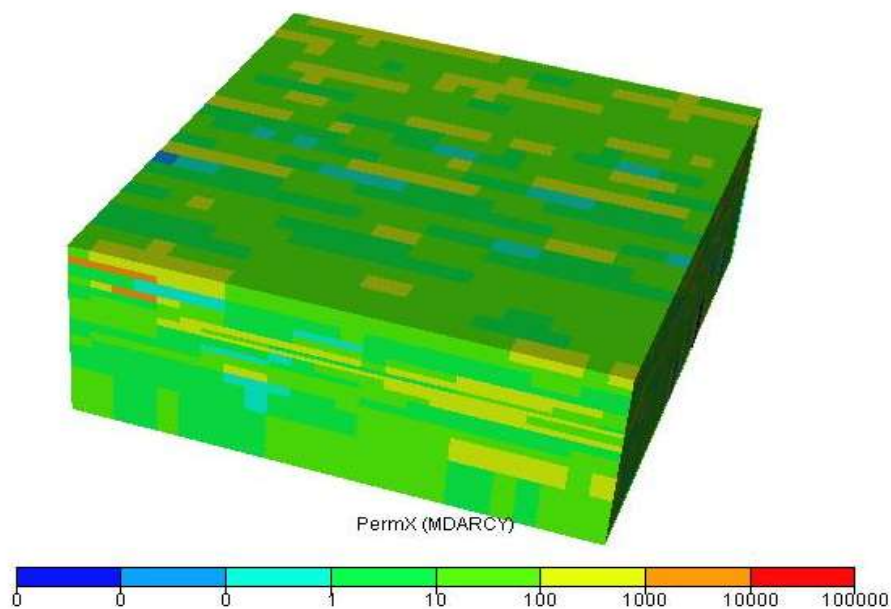


Figure 3.3: Horizontal permeability distribution within the reservoir

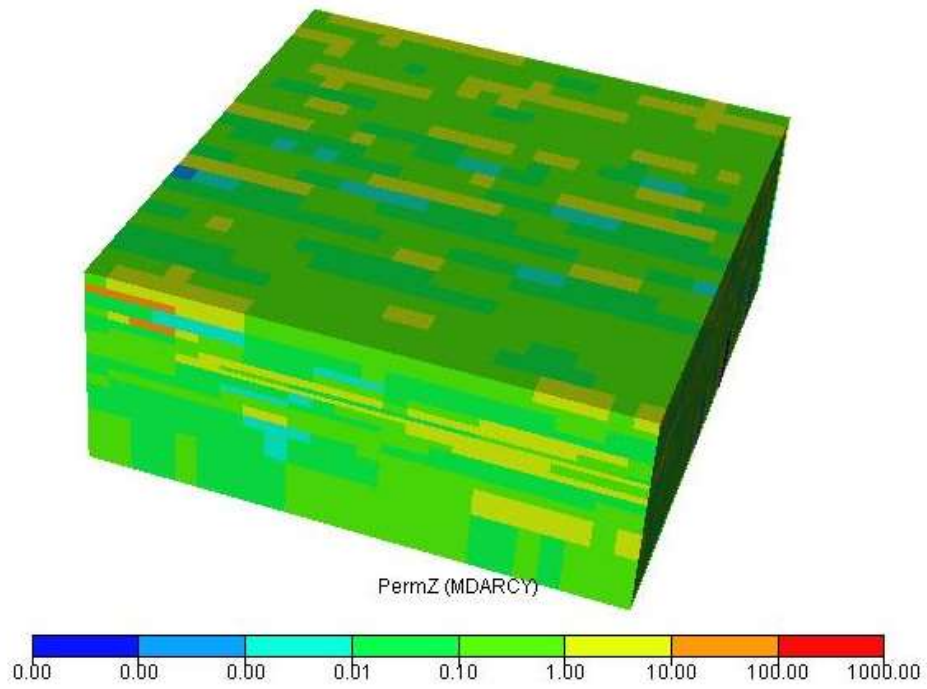


Figure 3.4: Vertical permeability distribution within the reservoir

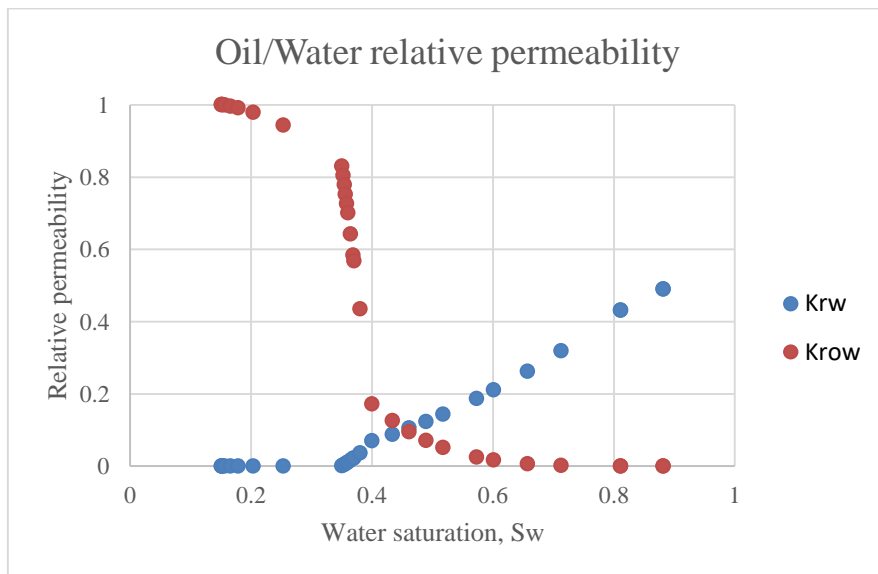


Figure 3.5: Oil and water relative permeability distribution

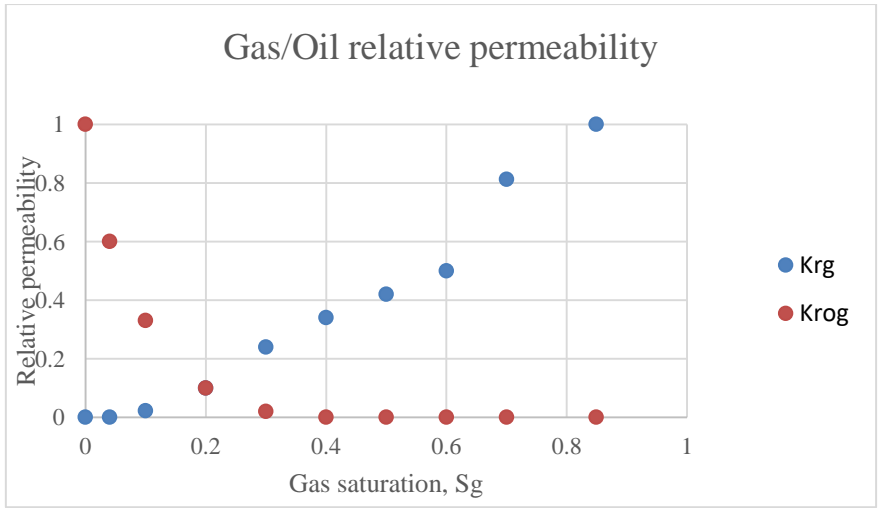


Figure: 3.6 Oil and water relative permeability distribution

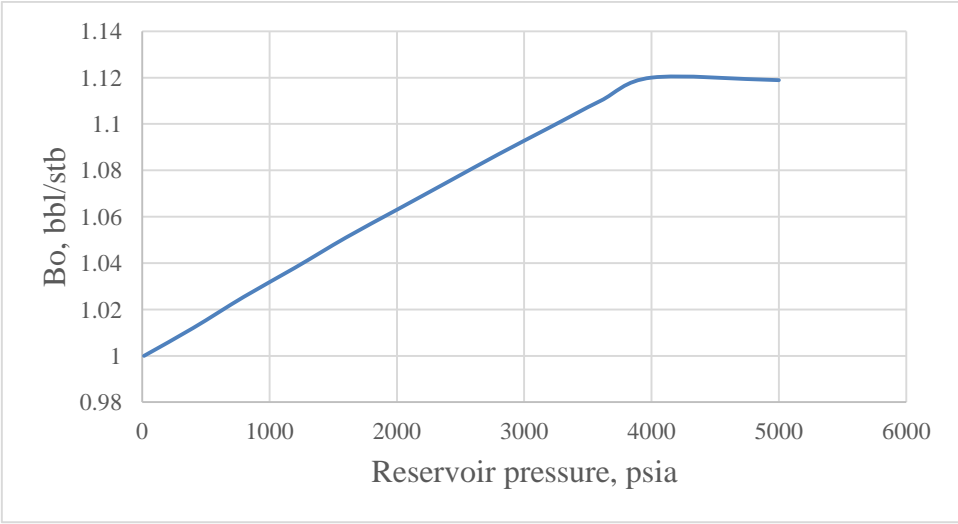


Figure 3.7: Variation of oil formation volume factor

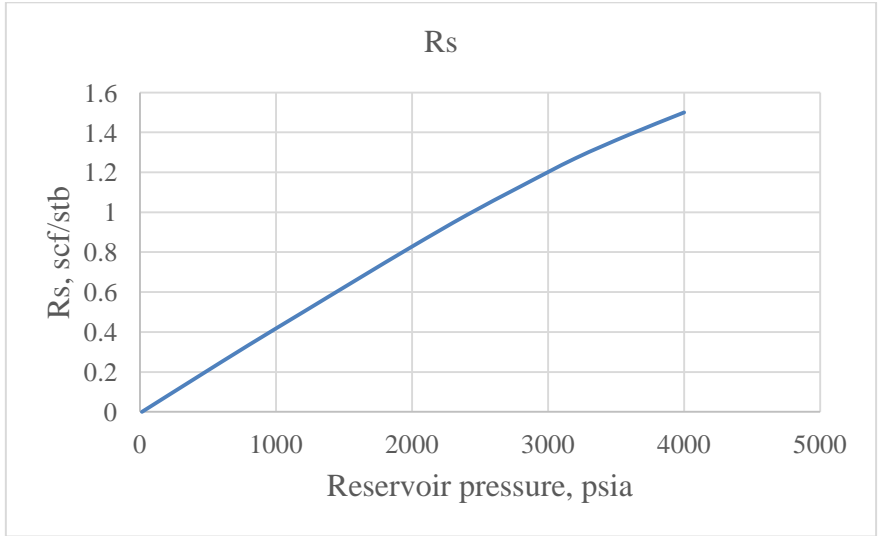


Figure 3.8: Variation of solution gas/oil ratio with pressure

The production of two vertical wells has been ongoing since 1980 but, after ten years, the cumulative oil production was observed to be underperforming. Therefore, after work on the wells and infill drilling using vertical wells, it was decided to define new horizontal wells to enhance the production of the field.

3.2 Determination of Initial Infill Well Location

In this study, the initial infill wells' location was determined using a space-filling design called the translational propagation Latin hypercube design (TPLHD). Here, the TPLHD was used because of its favourable properties such as good space filling performance occasioned by its ability to fill up the design space at the minimum distance (Vu et al., 2015 Guang Pan et al., 2014). This property is extremely important because it helps in capturing all variations evenly over the entire reservoir region. The TPLHD used was based on constructing an n-dimensional Latin hypercube design (LHD) from a relatively small optimal n-dimensional LHD design. Here, the designed TPLHD is a 15 by 2 design based on two variables (X and Y coordinates) and 15 sampling points. These sampling points represent the proposed location of the infill wells. This algorithm was originally designed by Viana et al. (2009) but was modified by using MATLAB[®] to suit the objective of this study. The underlying principles guiding the use of TPLHD in generating the initial infill wells' location is shown in Figure 3.8. During this search, rate allocation (as described in Section 3.3) for individuals was carried out using the oil and water production rates coupled with the bottomhole flowing pressure maintenance as a basis.

3.3 Well Rate Allocation Using Water Cut and Oil Cumulative Production

In order to control recovery processes aimed at improving the recoverable reserves from any field, reservoir management is a key task (Thakur, 1996). Control of any recovery process is through designing a well operating under time-varying pressure or production rate (Mojtaba et al., 2017). Most reservoir management approaches study the alleviation of the effect of excessive water cuts, gas injection, electric submersible pumps and infill drilling operations necessary to maximize recovery efficiency while maintaining the field pressure (FPR) at a moderate level (Mojtaba et al., 2017).

Determination of initial well location always comes with its associated optimization problems that result from the well completion and production data. When flow interactions between different wells are not significant, the well performance can be analyzed individually (Wang, 2003). In order to correctly determine the near-optimal rate required to maximize the available reserve, this section aims to develop an approach towards optimizing the target of cumulative oil and gas production, water cut and field pressure by varying the crude oil production rate while limiting the maintaining of field pressure decline and water cut occasioned by drilling new wells.

In this section, three scenarios (Cases 1, 2 and 3) were studied. Here, near-optimal production rates were studied by varying the production rate of each horizontal well (WOPR) from a high value with a high resultant pressure drop to nearly half its original value to study the effect on both the fields' and wells' cumulative oil production (FOPT and WOPT), water cut (FWCT and WWCT) and flowing pressure (WBHP and FPR). All of these scenarios were studied for approximately 20 years to assess their impact on outputs such as FOPT, FPR, WWCT, WOPT, WOPR and WBHP. The case descriptions are as follows:

Case 1

In this scenario, all of the fifteen horizontal wells were opened and operated at a limiting rate of 1500 STB/day at a bottomhole flowing pressure of about 500 psi.

Case 2

As shown in Table 3.1, after studying the time-varying behaviour of both the rate and pressure occasioned by Case 1, each horizontal well was produced at different rates.

Case 3

The reduction in the production rate of each well from Case 1 to Case 2 by half did not produce the optimal rate. The crude oil production rate of each well was further reduced by around half in order to study the resultant effect on field pressure and well water cut.

Table 3.1: Oil production rate (ORAT) of each horizontal well as used in Cases 2 and 3

Wells	ORAT (Case 2)	ORAT (Case 3)
1	800	400
2	400	200
3	600	400
4	600	350
5	300	200
6	300	200
7	400	300
8	400	200
9	500	300
10	200	100
11	300	150
12	50	50
13	500	300
14	400	200
15	600	400

3.4 Determination of the Optimum Number of Wells

In this work, the optimum number of wells and their corresponding positions can be estimated using reservoir fluid flow simulation based on the space-filling modelling design, that is, TPLHD with a special focus on minimizing the Euclidean distance between points in geometric space rather than using the uniform design used by Naderi et al. (2017). Fifteen different simulation designs using the geometric property of each horizontal well (x and y) were performed with other parameters such as horizontal well heel, length and direction maintained at the base level of oil zone midpoint, 1200 ft and 900 ft respectively, in other words, kept constant operating under the reservoir and production constraints as shown Table 3.1. A reservoir numerical simulation tool, Eclipse[®] 100 black oil was used to obtain important information such as cumulative oil production, gas production, water injection and water production. The measure of the index used in obtaining the optimum number

of wells and location is based on the economic parameter called normalized net present value, obtained using Equations 3.1 and 3.2.

$$NCF_t = (FOPT \times Oilprice) + (FGPT \times Gasprice) - (FWPT \times WHC) - (FWIT \times WIC) - TC \quad 3.1$$

$$NPV = \sum_{t=0}^{20} \frac{NCF_t}{(1+r)^t} \quad 3.2$$

$$NNPV = \frac{NPV - NPV_{min}}{NPV_{max} - NPV_{min}} \quad 3.3$$

Where:

FOPT = Field oil production total in STB

FGPT = Field gas production total in MSCF

FWPT = Field water production total in STB

FWIT = Field water injection total in STB

Oil price = \$50 per STB

Gas price = \$ 3.5 per MSCF

WIC = Water injection cost per bbl at \$2 per bbl

WHC = Water handling cost per bbl at \$2 per bbl

TC = Total drilling, surface equipment and short run maintenance cost at \$5MM per well

NPV = Net present value

NNPV = Normalized net present value

NPVmin = Minimum net present value

NPVmax = Maximum net present value

r = Discount rate at 0 %, 10 % and 20 %

t = time in years.

3.5 Surrogate Model Development

Running simulations for all possible sample locations within the reservoir search space can be computationally challenging (Anthony, 2014). Employing surrogate models or metamodels has been a popular technique for reducing the processing load in any optimization problem. The surrogate model approximates response behaviour and could be of the following forms, namely, quadratic, polynomial, multiplicative, kriging and radial basis function models as used in this work. Most

surrogate models require a set of initial points necessary to generate the model formulation. The initial points were generated using an experimental design approach called D-optimal.

The purpose of this section is to develop a surrogate model to forecast the horizontal well performance in a highly heterogeneous and anisotropic field. In this work, the objective function used is the net present value of the investment after 20 years of production. Parameters considered in the meta-modelling include the heel of the horizontal well (A), horizontal well length (B) and well direction (C). The reservoir model used was found to be highly heterogeneous and anisotropic, based on the Dykstra-Parsons coefficient and reservoir properties distribution respectively.

In this approach, parameters A, B and C were selected because the well geometric positions (x and y) were already optimized using the space-filling design techniques. As stated earlier, the heel of the horizontal well (A) is the point at which the well changes from a vertical to a deviated well, and the length of the well (B), which represented the extent of the well penetration, was coded using the number of grid blocks either in the x or y direction.

Finally, the horizontal well direction, denoted by variable “C”, is a discrete parameter that cannot be introduced into the Eclipse reservoir simulator directly but can be represented using an approach similar to Mohammadi et al.’s (2012), as shown in Figure 3.9 and interpreted using Table 3.2.

Table 3.2: Interpretation of well direction coding

Direction (degree)	Direction (rad)	Effect on x axis	Effect on y axis
45 ⁰	1	I	j + 1
90 ⁰	2	i + 1	j + 1
135 ⁰	3	i + 1	J
180 ⁰	4	i + 1	j – 1
225 ⁰	5	I	j – 1
270 ⁰	6	i – 1	j – 1
315 ⁰	7	i – 1	J

360°	8	$i - 1$	$j + 1$
-------------	---	---------	---------

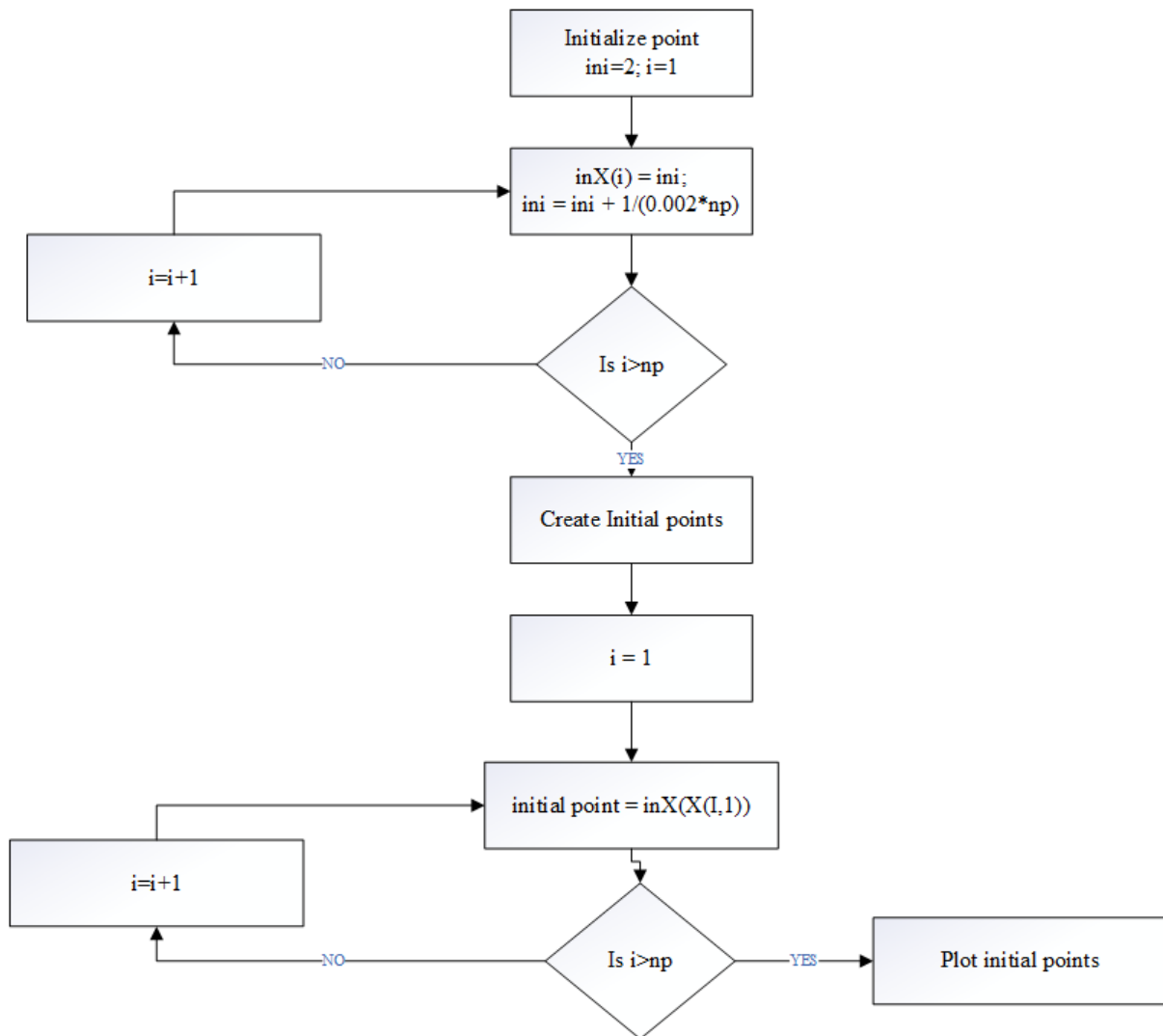


Figure 3.8: Frameworks for generating initial wells' location

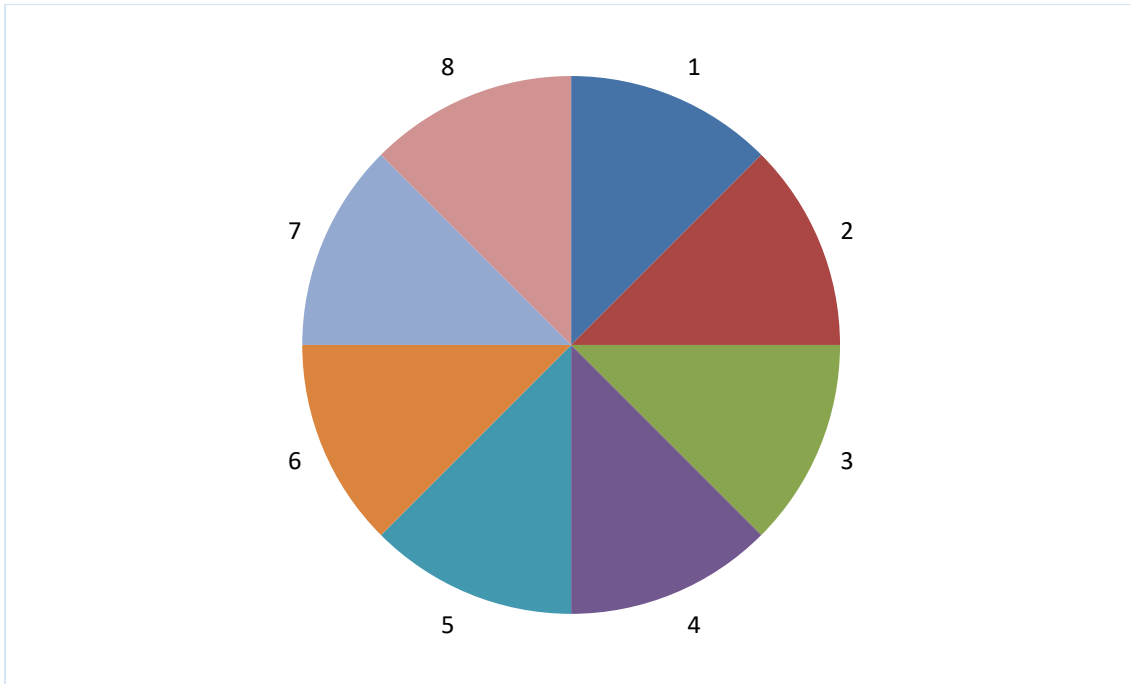


Figure 3.9: Horizontal well direction coding

3.5.1 Quadratic Approach

This method has been found to be useful in smoothing out noise associated with data measurement. The regression equation (Equation 3.4) developed was based on the outcome of the simulation response obtained using Eclipse® black oil simulator. In this model, the main and interaction effects are set out in Equation 3.4.

$$NPV = b_1 + b_2 \times A + b_3 \times B + b_4 \times C + b_5 \times A^2 + b_6 \times B^2 + b_7 \times C^2 + b_8 \times (A \times B) + b_9 \times (A \times C) + b_{10} \times (B \times C) \quad 3.4$$

The constants $b_1 - b_{10}$ were obtained using MATLAB® software based on the initial points obtained using D-optimal techniques.

3.5.2 Polynomial Approach

This model is similar to the quadratic model but has an additional interaction term to account for the smooth error. In this research, the polynomial model (Equation 3.5) was fitted using MATLAB® and constants ($b_1 - b_{11}$) determined using the existing initial points.

$$NPV = b_1 + b_2 \times A + b_3 \times B + b_4 \times C + b_5 \times A^2 + b_6 \times B^2 + b_7 \times C^2 + b_8 \times (A \times B) + b_9 \times (A \times C) + b_{10} \times (B \times C) + b_{11} \times (A \times B \times C) \quad 3.5$$

3.5.3 Multiplicative Approach

This model is similar to both the quadratic and polynomial models but it approximates the response by emphasizing the interaction between all the selected input parameters rather than the main effects, in other words, the multiplicative model considers all the parameters as one entity. In this research, the multiplicative model was regressed using Equation 3.6 with the aid of the MATLAB® simulation tool.

$$NPV = b_1 + b_2 \times (A^{b_3} \times B^{b_4} \times C^{b_5}) \quad 3.6$$

Where $b_1 - b_5$ are factors determined using Levenberg-Marquardt least-squares minimization approach in MATLAB®.

3.5.4 Kriging-based approach

Kriging is different from most RSMs because it is an interpolation technique that features data at sample locations (Zhong-Hua & Zhang, 2012). The kriging model assumes points are spatially correlated to one another with its estimated response being data exact. For this work, the kriging model was fitted using the Gaussian simulation approach because of its ability to account for noise inherent in most data measurements. The kriging model was fitted using MATLAB® and JMP statistical tools based on Equations 3.7 - 3.11 below.

$$NPV = f(\beta, X) + z(X) \quad 3.7$$

$$NPV = \beta f(X) + z(X) \quad 3.8$$

$$\beta = [\beta_1 \beta_2 \beta_3 \dots \beta_m]^T \quad 3.9$$

Where

β = regression function matrix which can be either constant, linear or quadratic model. Note: Constant type was used.

m = number of sample points being studied

X is a function of the selected parameters, i.e. A, B and C.

$z(X)$ = stochastic process with zero mean and nonzero covariance of the Gaussian type was used, due to their ability to model approximately the spatial variation of variables. The spatial covariance between points is given as:

$$E[z(X_i), z(X_j)] = \sigma^2 R[\theta, X_i, X_j] \quad 3.10$$

R = correlation matrix function between two sets of input variables at points X_i and X_j . The Gaussian correlation used is given as

$$R[\theta, X_i, X_j] = \exp \left[- \sum_{k=1}^m \theta_k |X_i - X_j|^2 \right] \quad 3.11$$

3.5.5 Radial Basis Function (RBF) Model

RBF is mathematically similar to the kriging-based approach. RBF is also an important interpolation technique as it approximates the desired response at untried locations using the linear combination of two functions, namely, radial basis and global trend. In this research, the RBF model was regressed using Equations 3.12 – 3.14 with the aid of the MATLAB[®] simulation tool.

$$NPV(x) = \sum_{i=1}^m v_i X(x) + N(x) \quad 3.12$$

subject to the following constraints:

$$y(x^i) = y^i, i = 1, 2, 3 \dots m \quad 3.13$$

$$\sum_{i=0}^m v_i = 0 \quad 3.14$$

where:

$X(x)$ = basis function which is a function of geometric distance (d) between the point of interest x^i and untried point x which can be of parameters A , B or C . Different basis based on any variable (i) are as follows:

Biharmonic $X(x) = d_i$

$$\begin{aligned} \text{Multiquadric:} \quad & X(x) = \sqrt{d_i^2 + c^2} \\ \text{Inverse Multiquadric:} \quad & X(x) = \frac{1}{\sqrt{d_i^2 + c^2}} \\ \text{Polyharmonic:} \quad & X(x) = (d_i^2 + c^2) \times \ln\left(\sqrt{d_i^2 + c^2}\right) \\ \text{Gaussian:} \quad & X(x) = \exp\left(\frac{-d_i^2}{2\delta^2}\right) \end{aligned}$$

3.5.6 Model Selection

To select a model that is truly representative of the nonlinear process being studied, the statistical approach was used to determine which of the surrogate models best mimics the interaction between the input and the response. The statistical tool used, as shown in Table 3.3, but not limited to absolute deviation (AD), average absolute deviation (AAD), root mean square error (RMSE), average absolute percentage relative error (AAPRE), maximum error (Emax) and standard deviation (SD), R-square values, fitting sequence and error band during prediction.

3.6 Optimization

In this research, the two metaheuristic algorithms used include the integer genetic algorithm (iGA) and the particle swarm optimization algorithm (PSO). Generally, GA is based on the Darwinian theory of evolution while PSO is based on the social and hunting behaviour of birds and fish when finding food while keeping in mind the dangers posed by predators.

In the iGA used, a set of individuals corresponding to the number of infill wells were randomly generated and the fitness of each solution were evaluated based on the already- developed surrogate models used to estimate their objective function, namely, NPV. Each solution was then evaluated to determine one with high NPV to be selected in the formation of a new population using both the crossover and mutation operators. These iteration steps continued until the stopping criterion was reached. The parameters used for the genetic algorithm are given in Table 3.4.

Similar parameters were used in the PSO algorithm used. In a typical PSO algorithm, determining the particles' position and velocity is key to obtaining an acceptable result. As earlier stated, a particle refers to a well location. In PSO, updating both the particle's position and velocity is a key step in achieving an optimal solution, but in updating this, three key factors, namely, inertia, self-confidence (social) and swarm confidence (cognitive) factors, must be correctly specified. In this research, the aforementioned parameters are listed in Table 3.4 and 3.5.

Table 3.3: Performance indices for model evaluation (Arinkoola & Ogbe, 2015)

Name of measure	Formula
Absolute deviation	$AD = \frac{1}{N} \sum_{i=1}^N (Pred. - exp.)$
Average absolute deviation	$AAD = \frac{1}{N} \sum_{i=1}^N Pred. - Exp. $
Root mean square error	$RMSE = \sqrt{\frac{1}{N} \sum_{i=1}^N (Pred. - Exp.)^2}$
Average absolute percentage relative error	$AAPRE = \frac{1}{N} \sum_{i=1}^N (Pred. - Exp.)_i $
Maximum error	$E_{max} = Max (Pred. - Exp.)_i $ $E_{min} = Min (Pred. - Exp.)_i $ $E_i = \frac{Pred. - Exp.}{Exp.} \times 100$
Standard deviation	$SD = \frac{1}{N - 1} \times \sum_{i=1}^N (Pred. - Exp.)_i^2$

Table 3.4: Selected genetic algorithm parameters

Parameters	Value
Population size	30
Crossover probability	0.8
Mutation probability	0.01
Stopping criteria	1000
Selection function	Stochastic uniform
Ranking scale	2

Table 3.5: Selected particle swarm optimization parameters

Parameter	Value
Population size	30
Inertia coefficient	1
Cognitive parameter	2
Social parameter	2
Stopping criteria	1000

CHAPTER FOUR: RESULTS AND DISCUSSIONS

The results from the initialization of the number and position of infill wells in a highly heterogeneous reservoir were generated using a space-filling design coupled with Eclipse[®] 100 black oil simulator and are presented below. Surrogate models were developed for the system based on a polynomial, kriging and radial basis function model. D-optimal design was used to generate initial data points for prediction. Metaheuristic-based optimization was carried out to determine the optimum value for the different parameters' effects on the desired response. As indicated earlier, the value of the objective function was maximized as earlier discussed.

4.1 Rate Allocation

In this research, before the optimization was carried out, production rates were allocated using water cut and cumulative oil production. The results of all the scenarios obtained, using this allocation approach, are presented in this section.

4.1.1 Analysis of Wells 1, 2, 3 and 4

Figures 4.1, 4.2, 4.3 and 4.4 show the profile of the crude oil production rate (WOPR), cumulative oil production (WOPT), bottomhole flowing pressure (WBHP) and water cut (WWCT) respectively for each of the first four horizontal wells using the rate allocation method, as described.

For Well 1, reducing the production rate resulted in a similar water breakthrough time, but a reduced WWCT for about 10 years and a slight change in WOPT and WBHP due to a high degree of heterogeneity characteristic of the reservoir. Wells 2, 3, and 4 show a similar trend to Well 1 but in Well 3, Case 3, with the lowest production rate, approximately matches that of Case 1 due to the presence of sufficient pressure support.

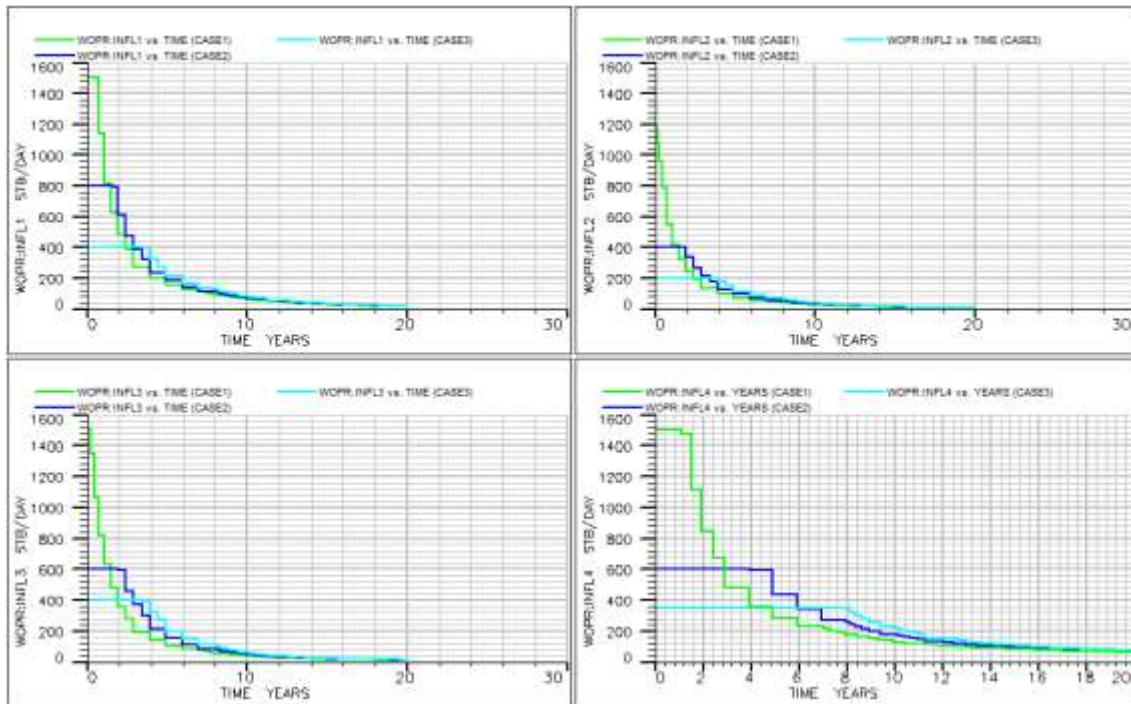


Figure 4.1: Crude oil production rate of Wells 1, 2, 3 and 4 for all cases

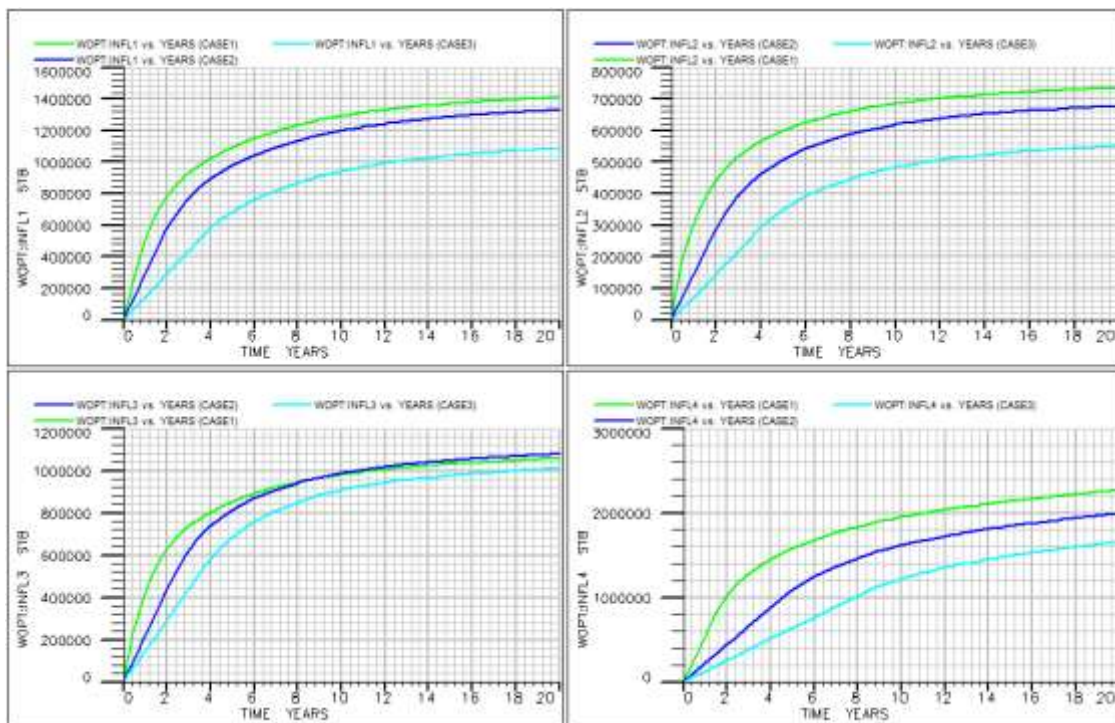


Figure 4.2: Cumulative oil production profile of Wells 1, 2, 3 and 4 for all cases

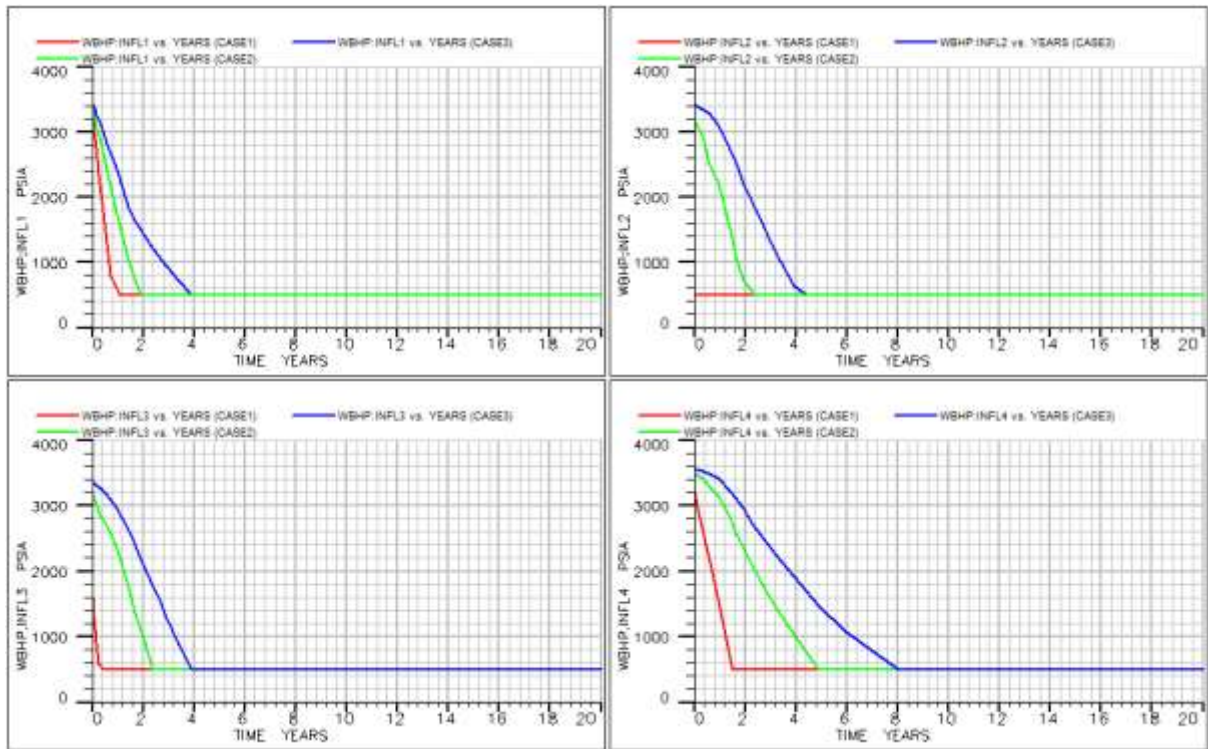


Figure 4.3: Bottomhole flowing pressure profile of Wells 1, 2, 3 and 4 for all cases

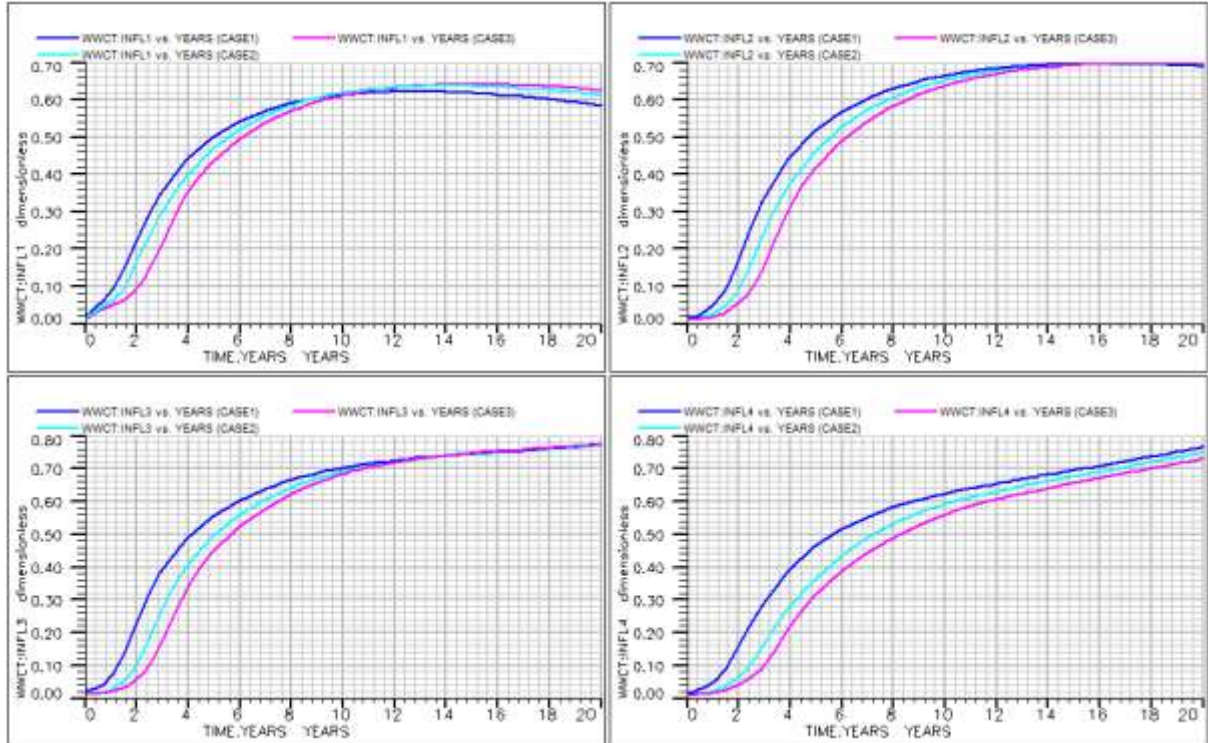


Figure 4.4: Well water cut profile of Wells 1, 2, 3 and 4 for all cases

4.1.2 Analysis of Wells 5, 6, 7 and 8

Figures 4.5, 4.6, 4.7 and 4.8 show the profile of the crude oil production rate (WOPR), cumulative oil production (WOPT), bottomhole flowing pressure (WBHP) and water cut (WWCT) respectively for four horizontal wells (INFL 5, 6, 7 and 8) using the rate allocation method as described. For Wells 5 and 6, reducing the WOPR did not significantly change the WOPT after 20 years but the plateau rate and WBHP were maintained at an appreciable level for about five years with a resultant reduction in WWCT for about 10 years. In contrast, reducing the oil production rate for Wells 7 and 8 had a significant effect on WOPT and a favourable WBHP maintenance with a corresponding reduction in WWCT for about 10 years.

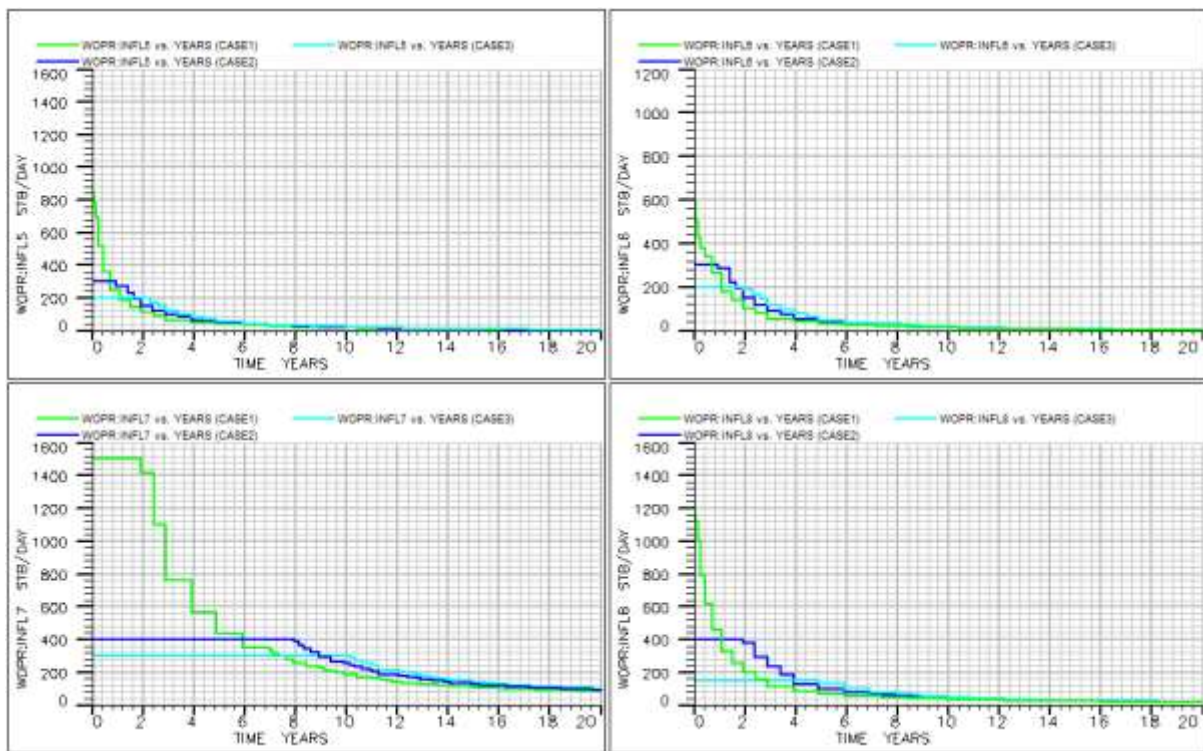


Figure 4.5: Crude oil production rate of Wells 5, 6, 7 and 8 for all cases

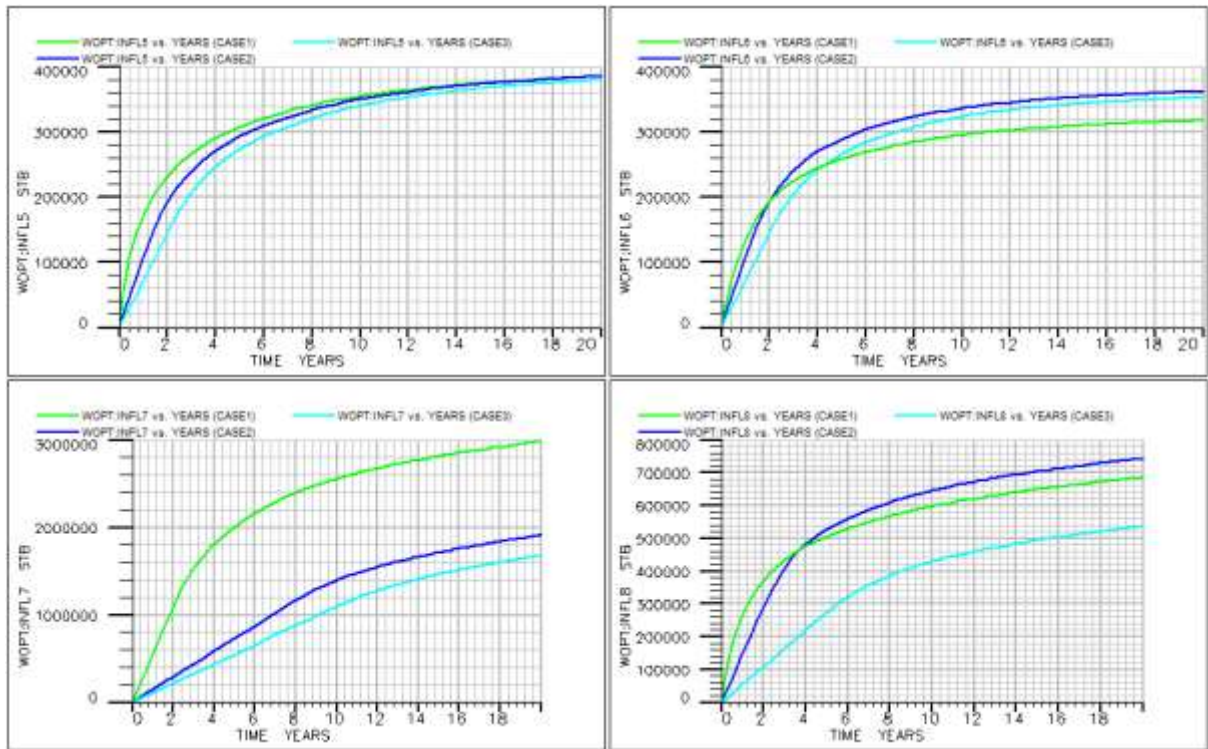


Figure 4.6: Cumulative oil production profile of Wells 5, 6, 7 and 8 for all cases

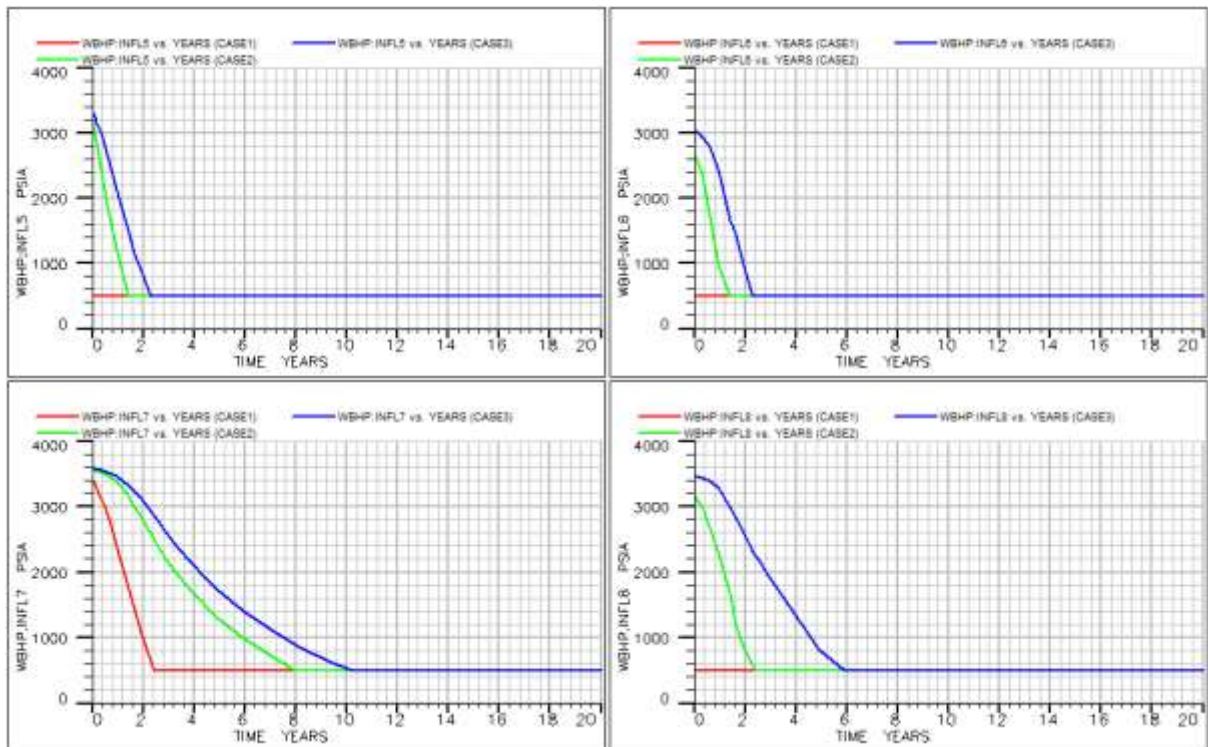


Figure 4.7: Bottomhole flowing pressure profile of Wells 5, 6, 7 and 8 for all cases

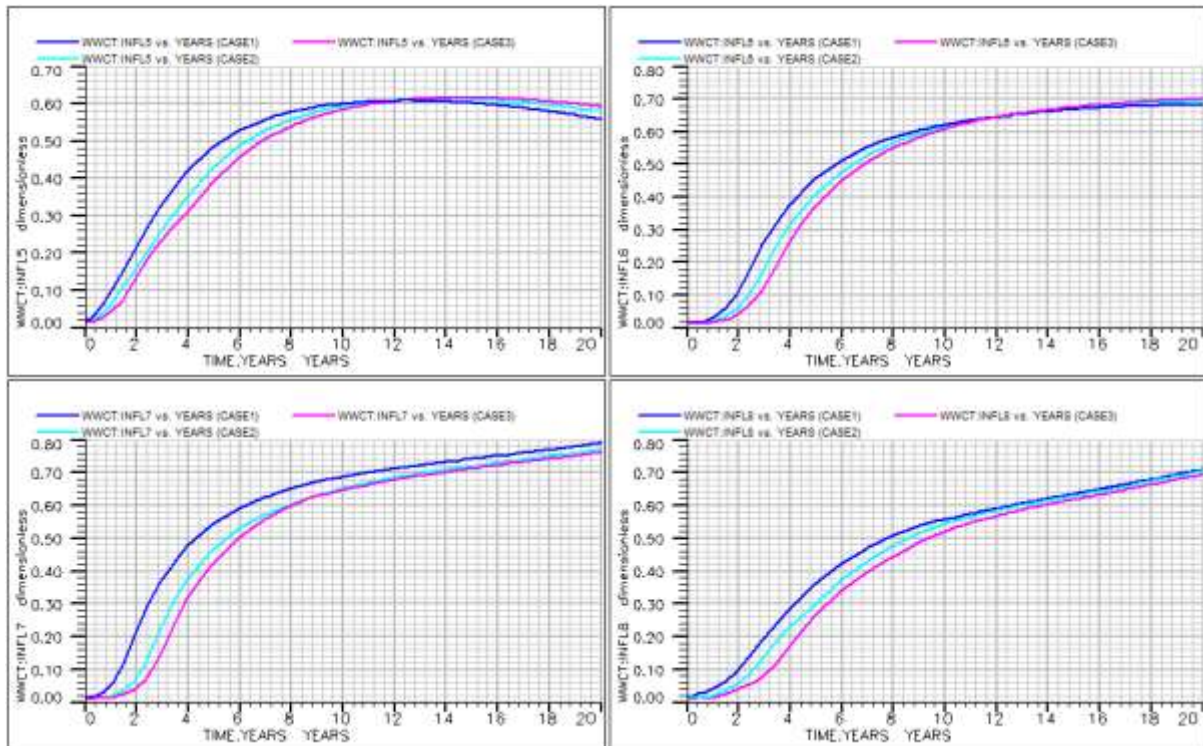


Figure 4.8: Well water cut profile of Wells 5, 6, 7 and 8 for all cases

4.1.3 Analysis of Wells 9, 10, 11 and 12

The results of the effect of crude oil production rate variation in estimating the near-optimal rate for wells are shown in Figures 4.9 - 4.12. Figures 4.9, 4.10, 4.11 and 4.12 show the profile of the crude oil production rate (WOPR), cumulative oil production (WOPT), bottomhole flowing pressure (WBHP) and water cut (WWCT) respectively for four horizontal wells (INFL 9, 10, 11 and 12) using the rate allocation method, as described. Reducing the WOPR of each well resulted in appreciable plateau rate maintenance. The resultant decrease in WOPT and significant improvement in pressure decline is shown in Figures 4.9, 4.10 and 4.11 respectively. In all scenarios shown in Figure 4.12, the WWCT trend of all wells shows a significant reduction in WWCT but a marked increase towards the end of production.

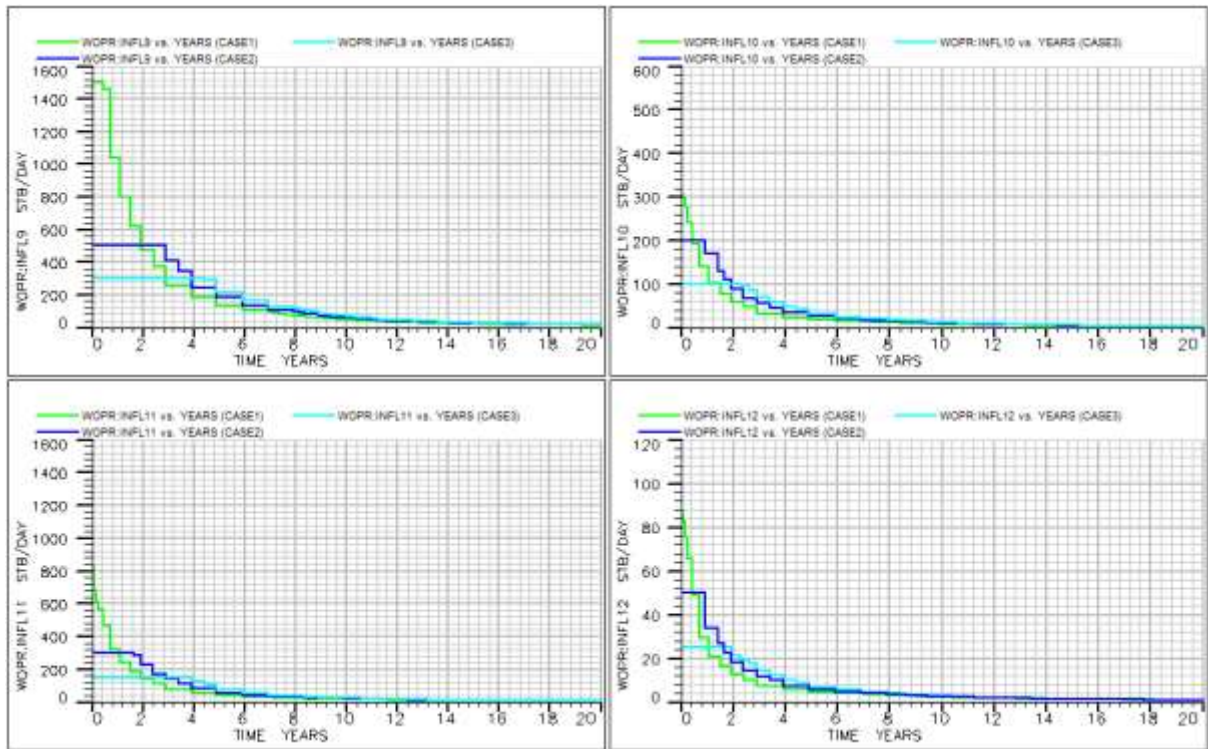


Figure 4.9: Crude oil production rate of Wells 9, 10, 11 and 12 for all cases

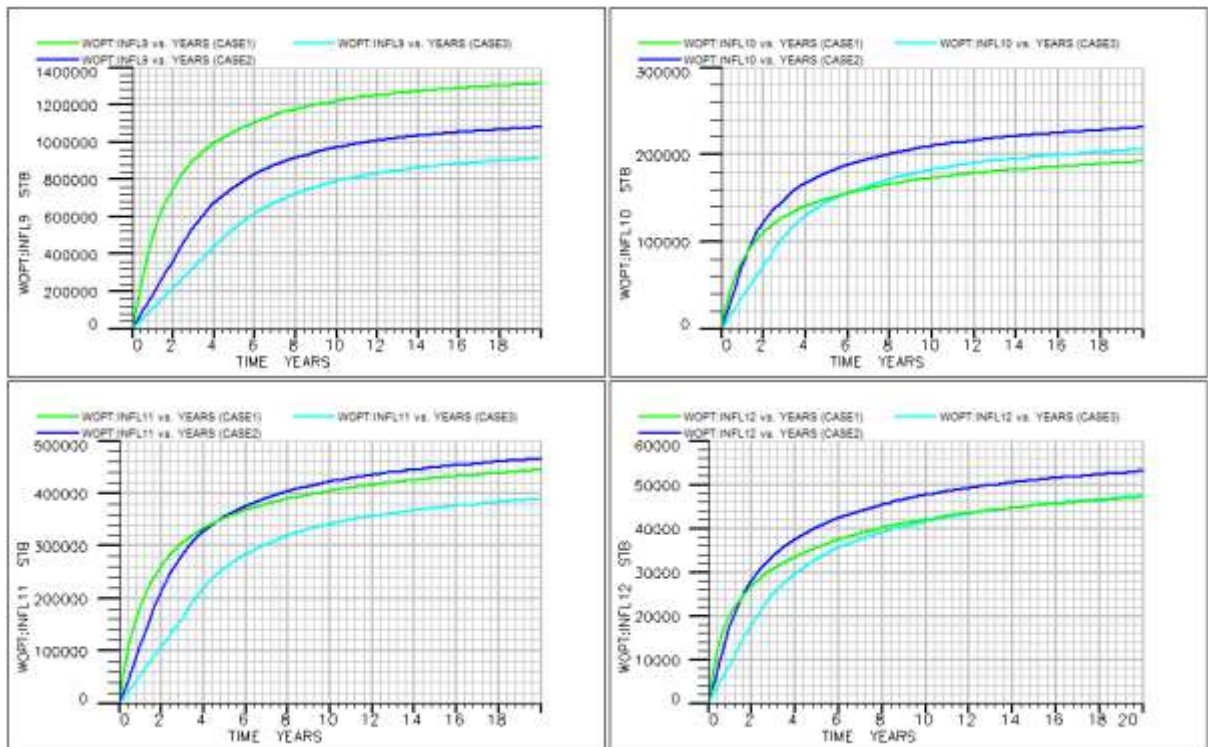


Figure 4.10: Cumulative oil production profile of Wells 9, 10, 11 and 12 for all cases

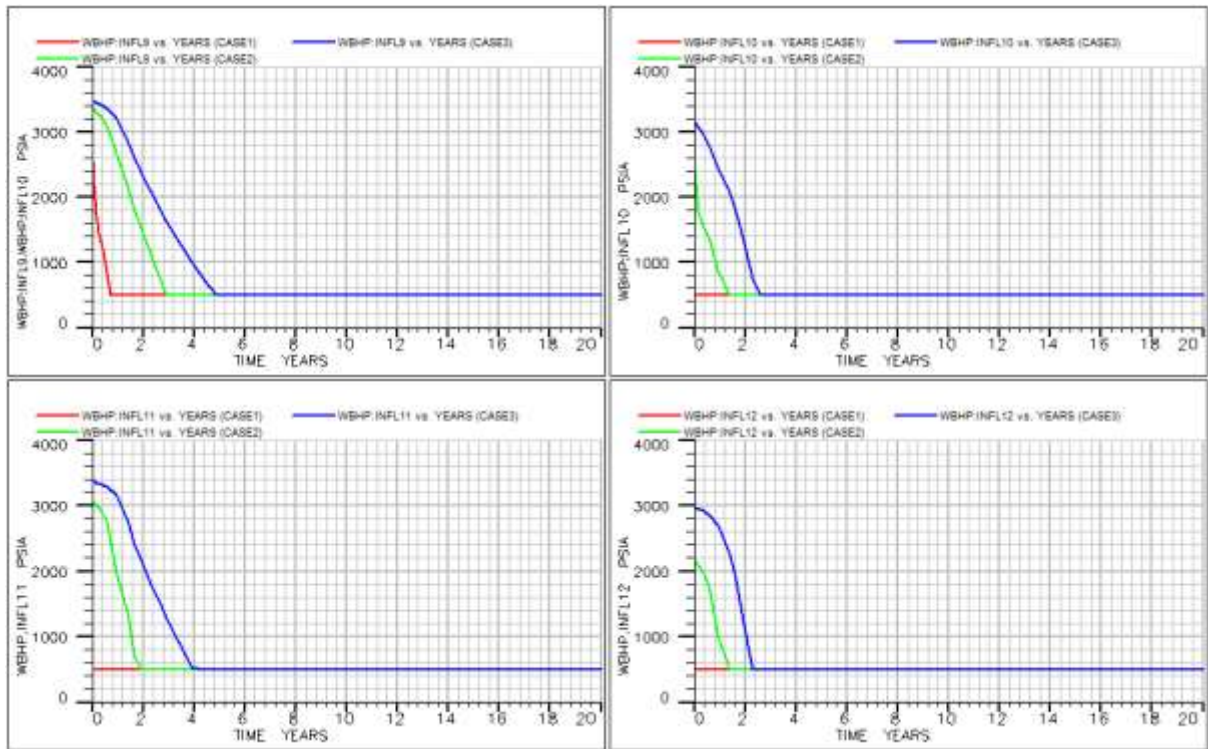


Figure 4.11: Bottomhole flowing pressure profile of Wells 9, 10, 11 and 12 for all cases

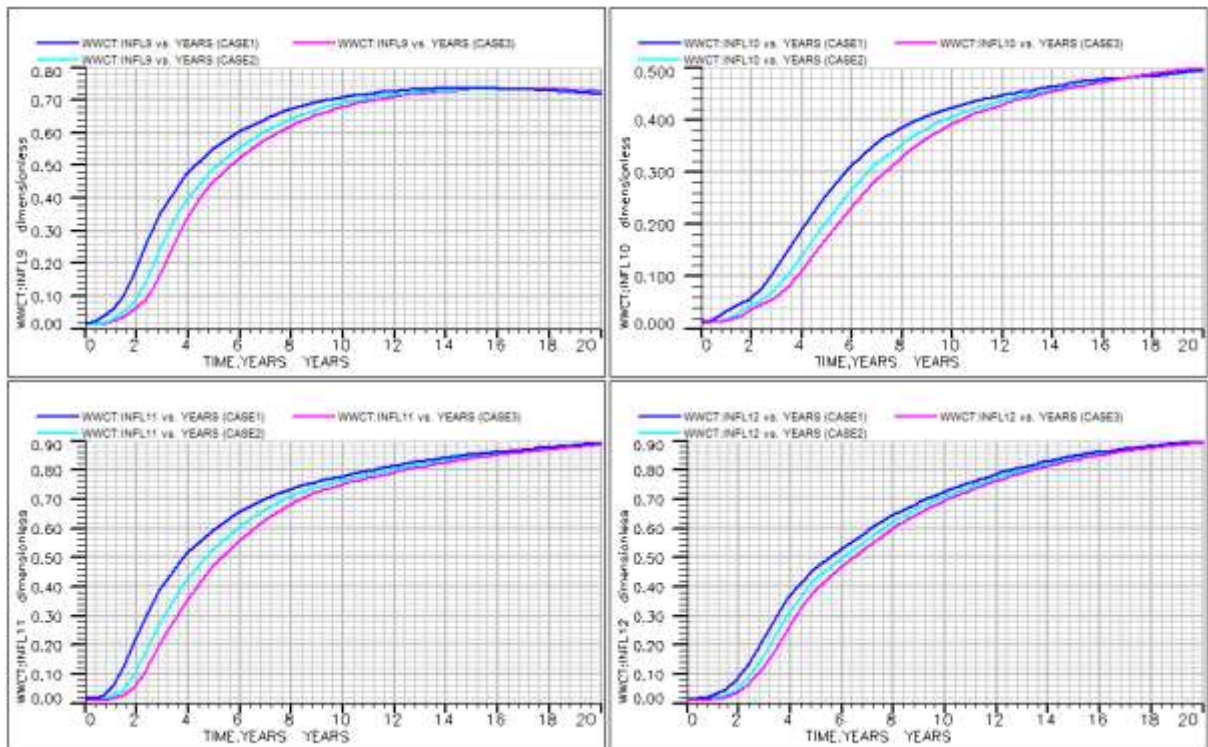


Figure 4.12: Well water cut profile of Wells 9, 10, 11 and 12 for all cases

4.1.4 Analysis of Wells 13, 14 and 15

Figures 4.13 – 4.16 show all the rate allocation studies of Wells 13, 14 and 15 using parameters WOPR, WOPT, WBHP and WWCT for all aforementioned scenarios. From the results, it was observed that Well 13 showed a small variation in the WOPT after 20 years with favourable BHP maintenance traits but reduced WWCT for the first 10 years, as shown in Figures 4.14, 4.15 and 4.16 respectively. In contrast, Well 14 shows a marked difference in WOPT but a reduced BHP decline compared to Well 13 as seen in Figures 4.14 and 4.15 respectively. For Well 15, reducing production rate resulted in a good plateau rate maintenance trend for about 10 years (Figure 4.13), but declined slowly afterwards. From its WBHP (Figure 4.15) and WWCT (Figure 4.16) trends, it was observed that its WOPR results reduced at a similar rate to Wells 13 and 14, but it had a significant pressure decline.

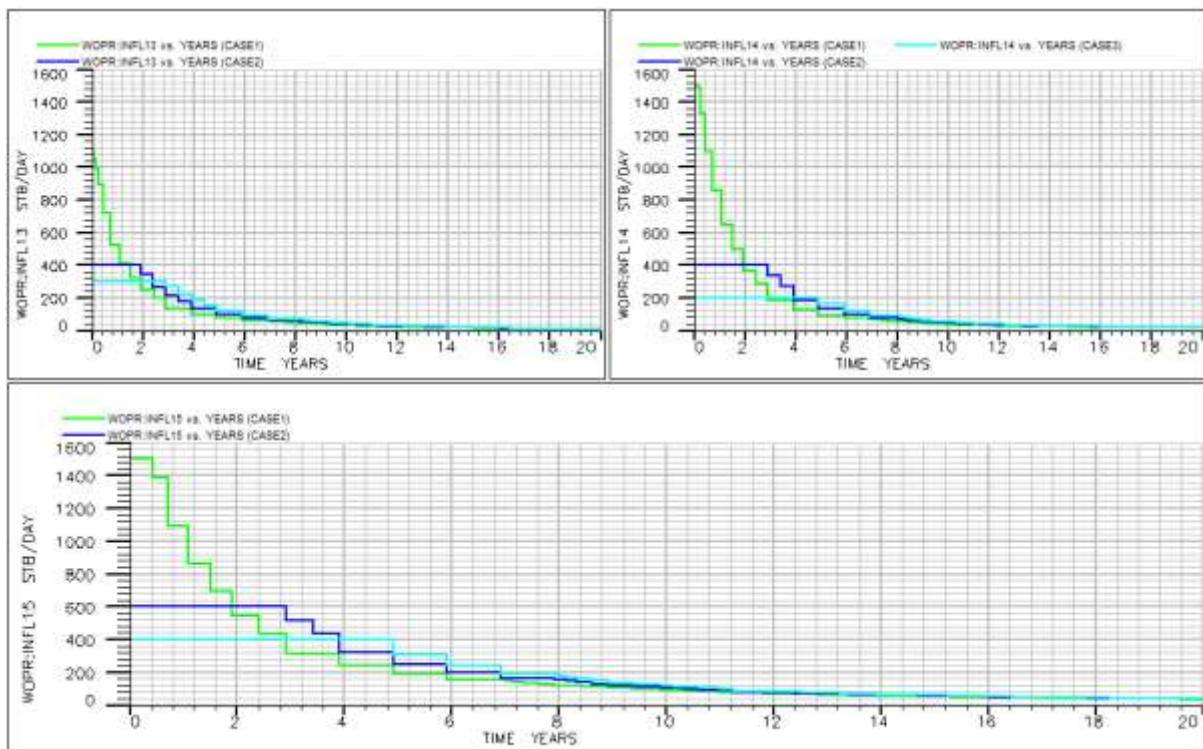


Figure 4.13: Crude oil production rate of Wells 13, 14 and 15 for all cases

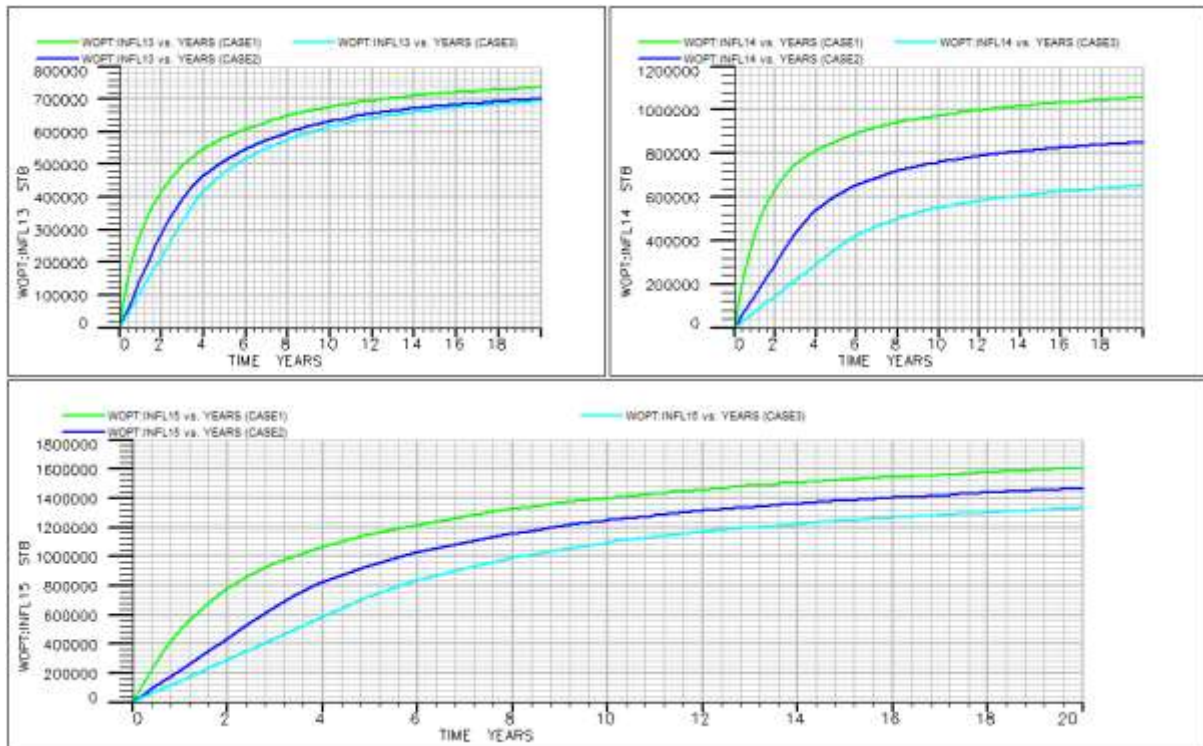


Figure 4.14: Cumulative oil production profile of Wells 13, 14 and 15 for all cases

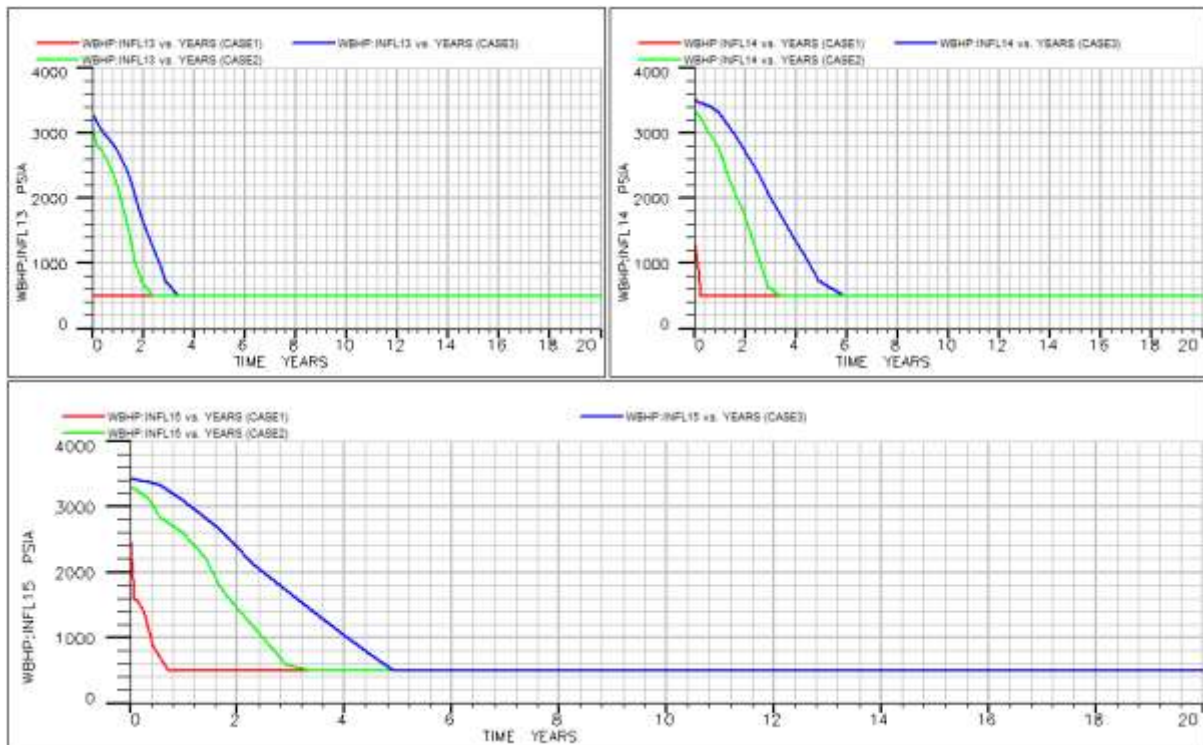


Figure 4.15: Bottomhole flowing pressure profile of Wells 13, 14 and 15 for all cases

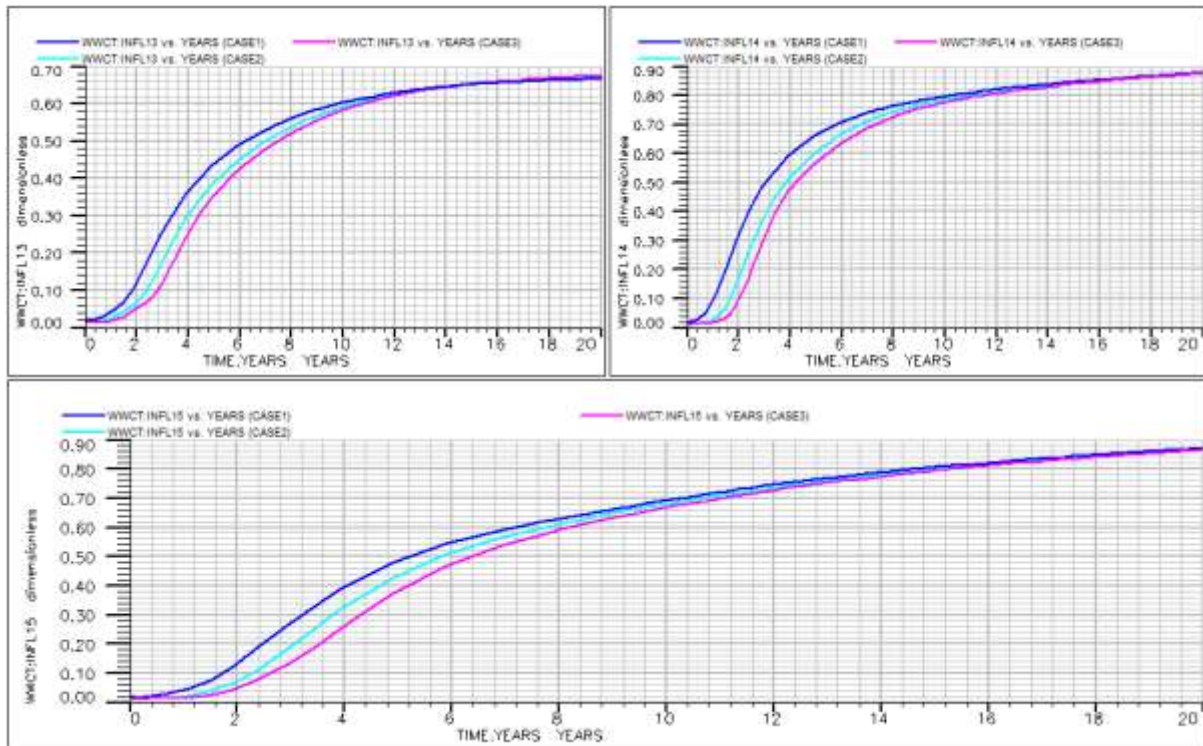


Figure 4.16: Well water cut profile of Wells 13, 14 and 15 for all cases

From the study of each well's performance on the basis of WOPR, WOPT, WBHP and WWCT, it was observed that, in order to maintain the field production at a near-optimal rate for a favourable number of years occasioned by a favourable WBHP, each of the 14 agile horizontal wells must be operated to give a higher FOPT while maintaining the FPR at an optimized decline rate as shown in Figure 4.17.

4.2 Well Placement Initialization and Maximization

In order to obtain the best Euclidean position of the additional infill wells required to give the maximum return on investment, the net present value (NPV) rather than the cumulative oil production was used as the desired objective function and maximized using an improved space-filling design coupled with a reservoir simulator. Executing the reservoir simulation based on the translational propagation Latin hypercube design suggests that both the undiscounted net present value (UNPV) and NPV were maximized for eleven horizontal wells, as shown in Figure 4.18, using the heterogeneous reservoir model as the case study. Figures 4.19 and 4.20 show the initial location and optimum location of the individual horizontal wells that were obtained using initial guess and TPLHD respectively, it was observed that increasing

either the number of wells or the discount rate would not affect the optimum number of wells of the studied scenario.

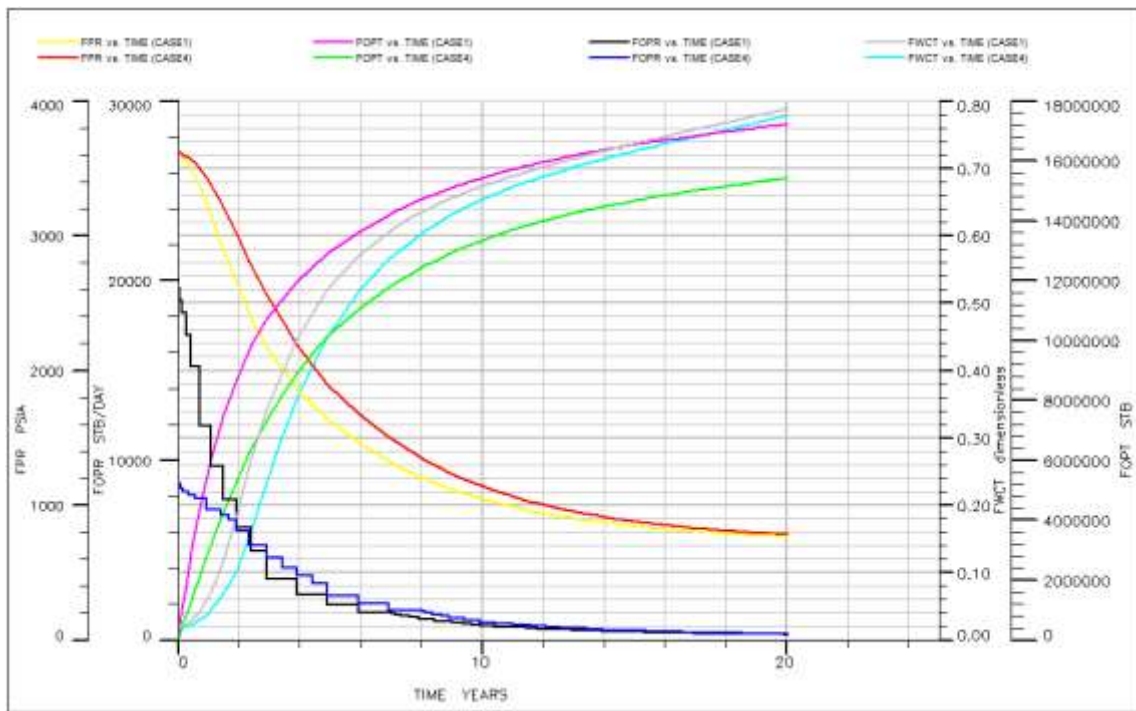


Figure 4.17: Recommended crude oil field production profile

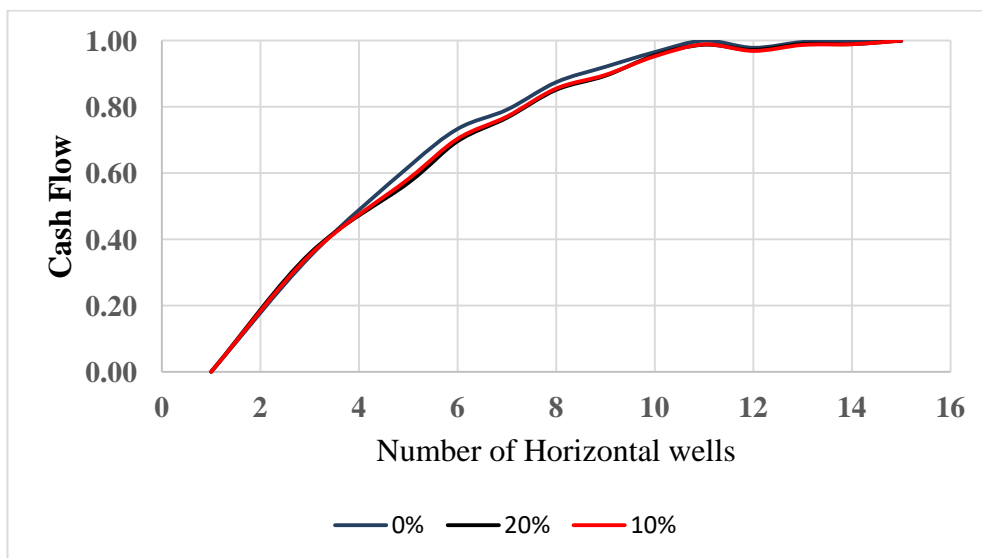


Figure 4.18: Results of simulation-based optimization using TPLHD design

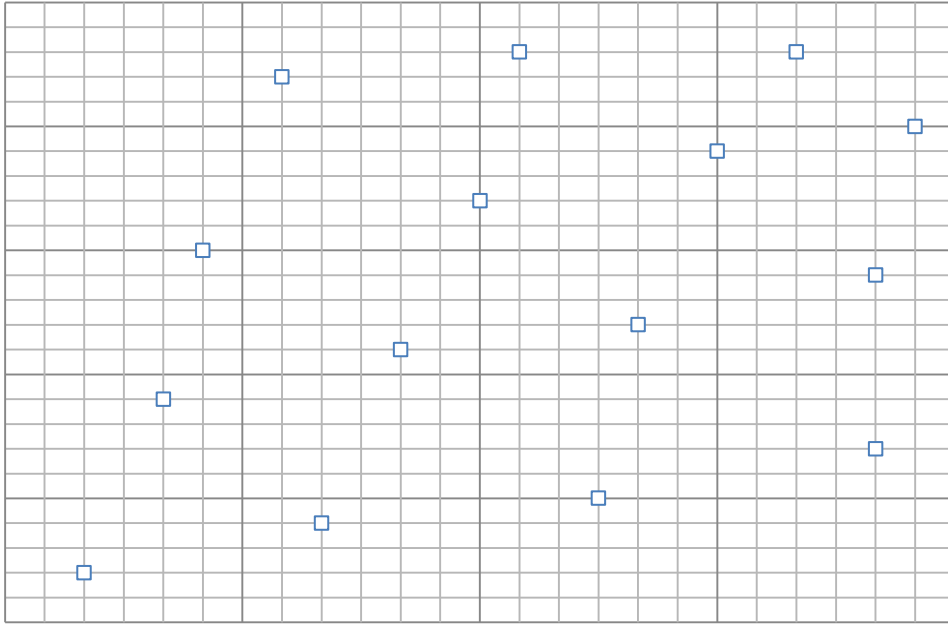


Figure 4.19: Wells' initial location based on TPLHD

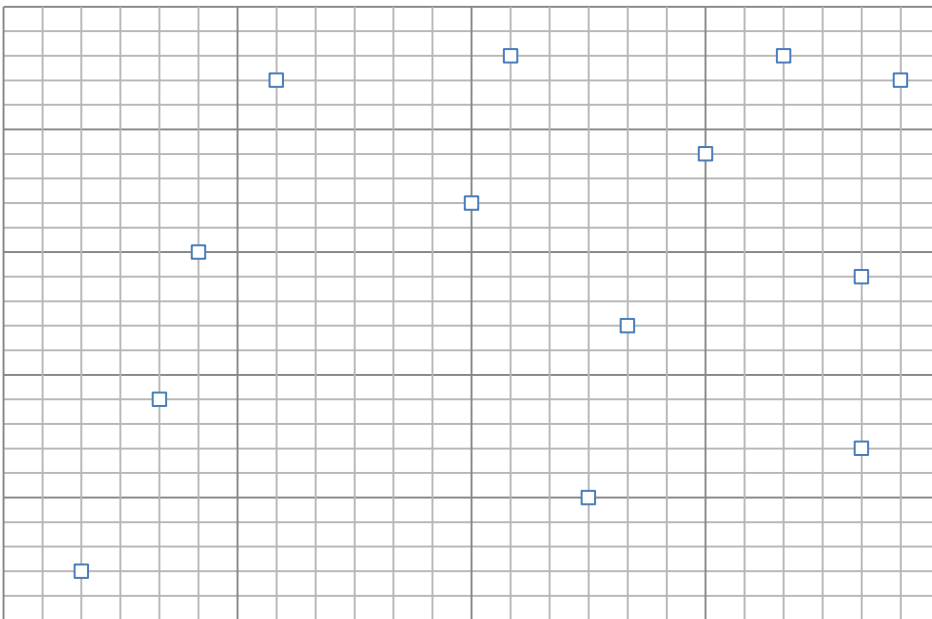


Figure 4.20: Optimum wells' number and locations

4.3 Surrogate Model

In this section, after the different production profiles had been converted to appropriate monetary values, based on the distribution of selected parameters obtained using the D-optimal design technique for each of the horizontal wells. Different surrogate models were developed using the method discussed in the

methodology. In the following section, the fitting and prediction performances are explained in relation to each well's surrogate.

4.3.1 Well 1

In this approach, the desired response, that is, NPV was fitted over approximately 85% of the sample data obtained from the simulation approach used. As it is this work's objective to determine the optimal completion strategy for each of the optimized horizontal wells, each surrogate model was developed as a function of each of the selected horizontal well parameters while maintaining other wells at their base case as obtained during maximization using space-filling design. Equations 3.4, 3.5 and 3.6 were used in obtaining quadratic, polynomial and multiplicative models for each of the horizontal wells. In addition, the Gaussian regression process and various radial basis functions, as outlined in the methodology, were used in the kriging and radial basis function approach fittings respectively. For Well 1, five different surrogate models were considered. Table 4.1 shows the statistical analysis performance of each model. The fitting and prediction performance of each surrogate model was compared with that of the simulator, as shown in Figures 4.21a and 4.21b respectively. For the quadratic, polynomial and multiplicative models, the constants obtained are shown in Table 4.1. Different colours depict the different proxy models' performance with black, blue, red, yellow, brown and green representing Eclipse® 100 simulator output, kriging, RBF, quadratic, multiplicative and polynomial respectively. In the kriging model, the variogram-based model, which has the best fit to the data outlined by Mohammadi et al. (2002), was chosen, while different basis functions were used in fitting the RBFs. To compare the model prediction with the actual data, the predicted and simulator response were plotted, as shown in both graphs. From the graph, it was observed that both kriging and RBF had the best fitting tendencies with the multiplicative being the poorest as buttressed by their least estimation error and highest values of correlation coefficients, as kriging is a data-exact estimator because they tend to replicate the actual response rather than force fitting. In the prediction graph (Figure 4.21b), it was observed that responses from some surrogate models did not match the actual value accurately but showed appreciable error because of the noisy nature of the data characteristic of the dataset. The kriging-based models were observed to perform better because of their ability to smooth out noise inherent in different data.

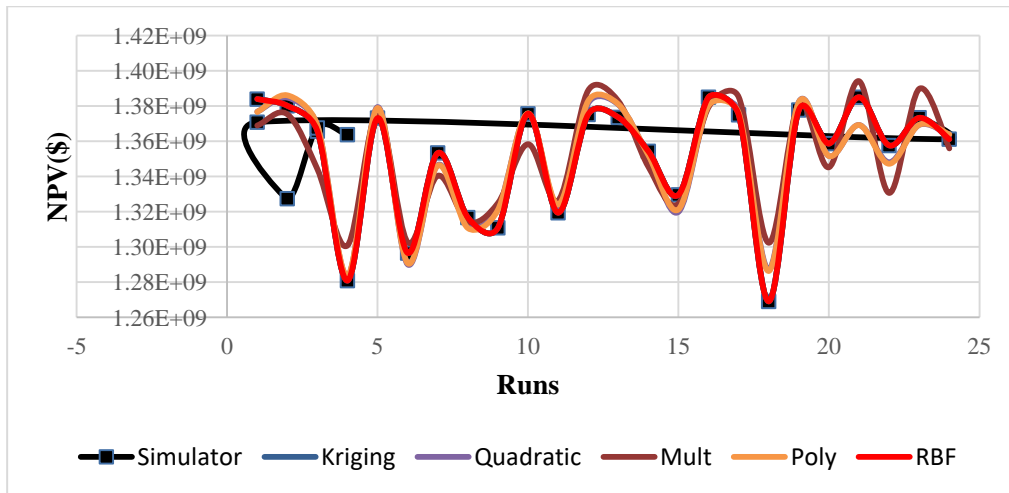


Figure 4.21a: Fitting results of surrogate models for Well 1 with selective initial points

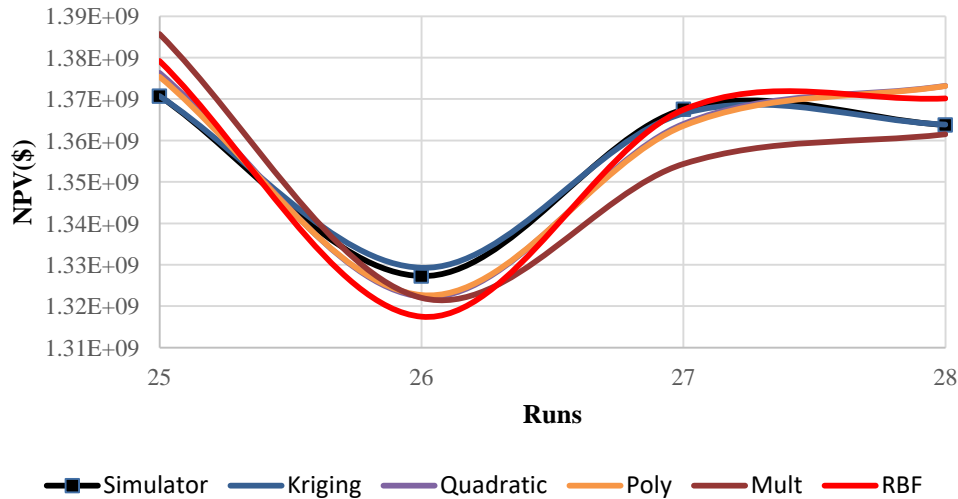


Figure 4.21b: Prediction results of surrogate models for Well 1 with selective initial points

Table 4.1: Summary of the performance indices of surrogate models for Well 1

Performance	Quadratic	Polynomial	Multiplicative	Kriging	RBF
AD	0.00	0.00	428.58	-39285.71	-177230.57
AAD	6195748.05	6226861.21	11411245.89	110714.29	884755.83
RMSE	7323398.06	7290447.11	13656344.36	422999.49	2730744.16
E _{max}	1.43	1.36	2.62	0.15	0.62
AAPRE	0.46	0.46	0.85	0.01	0.07
SD	0.31	0.31	1.09	0.00	0.04

R2_fitting	0.95	0.95	0.82	0.99	0.99
R2_Prediction	0.94	0.94	0.82	0.98	0.95

4.3.2 Well 2

An approach similar to that used for Well 1, was used for Well 2. Eclipse® 100 simulation data was used for model development. Three different polynomial-based surrogate models (quadratic, polynomial and multiplicative) as well as two geometric-based surrogate models (kriging and radial basis function) were considered for this research. For each of the selected response surface models, the results of the performance indices used are shown in Table 4.2. Similarly, to validate the different surrogate models developed, the models were used to estimate the objective function at points with known responses, and each response was compared with that of the simulator as shown in Figure 4.22b. For the quadratic, polynomial and multiplicative models, the constants obtained are shown in Table 4.2. The response (NPV) was then calculated using the weights obtained by solving kriging equations with the MATLAB® and JMP tools. Figure 4.22a shows the plot of actual and proxy estimates of the objective function over twenty years of cumulative production. Different colours depict the different proxy models' performances with black, blue, red, yellow, brown and green representing Eclipse® 100 simulator output, kriging, RBF, quadratic, multiplicative and polynomial models respectively. From Figure 4.22a, it was observed that both kriging and RBF have the best fitting tendencies with the multiplicative being the poorest and highest regression coefficients and least error. It should be noted that kriging is an exact estimator, which means the estimations of the kriging and RBF models for the initial sample points must be exact because they tend to replicate the actual response rather than force fitting (Mohammadi et al., 2012; Kentwell, 2014). Similarly, in the prediction phase, it was observed that responses from the surrogate models matched the actual value at an appreciable range as shown in Figure 4.22b with the kriging-based approach and multiplicative models having the best and worst fits respectively.

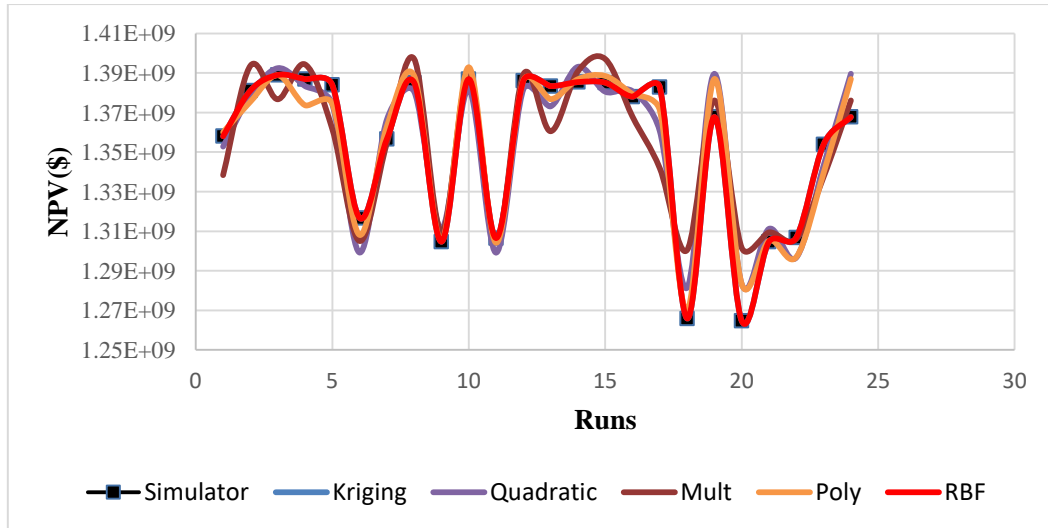


Figure 4.22a: Fitting results of surrogate models for Well 2 with selective initial points.

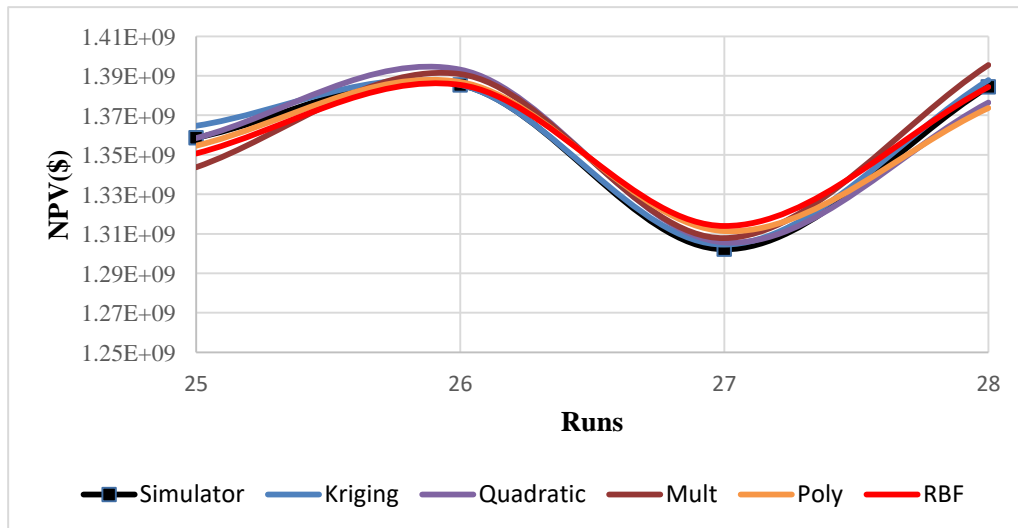


Figure 4.22b: Prediction results of surrogate models for Well 2 with selective initial points.

Table 4.2: Summary of the performance indices of surrogate models for Well 2

Performance	Quadratic	Polynomial	Multiplicative	Kriging	RBF
AD	0.00	0.00	355.73	-423912.98	-135727.65
AAD	8984505.48	6902271.10	12546830.47	423912.98	707422.50
RMSE	10915948.19	9033682.42	16309347.93	1390462.81	2692061.39
Emax	1.60	1.47	2.92	0.45	0.91
AAPRE	0.67	0.51	0.93	0.03	0.05
SD	0.69	0.47	1.55	0.01	0.04
R2_fit	0.96	0.97	0.91	0.99	0.99

R2_Pred	0.95	0.96	0.89	0.99	0.95
---------	------	------	------	------	------

4.3.3 Well 3

An approach similar to those above was used. Five different surrogate models were also considered. Table 4.3 shows the statistical analysis results while the fitting and prediction performance of each surrogate model was compared with that of the simulator, as shown in Figures 4.23a and 4.23b respectively. From Figure 4.23a, it was observed that both kriging and RBF have the best fitting tendencies with the multiplicative being the poorest, as indicated by the performance indices as shown in Table 4.3. In the prediction plot (Figure 4.23b), it was observed that responses from the surrogate models did not match the actual value accurately but showed appreciable error because of the noisy nature of the dataset. The polynomial-based models were observed to performed better because of their ability to smooth out noise inherent in different data but kriging and RBF had the best fit.

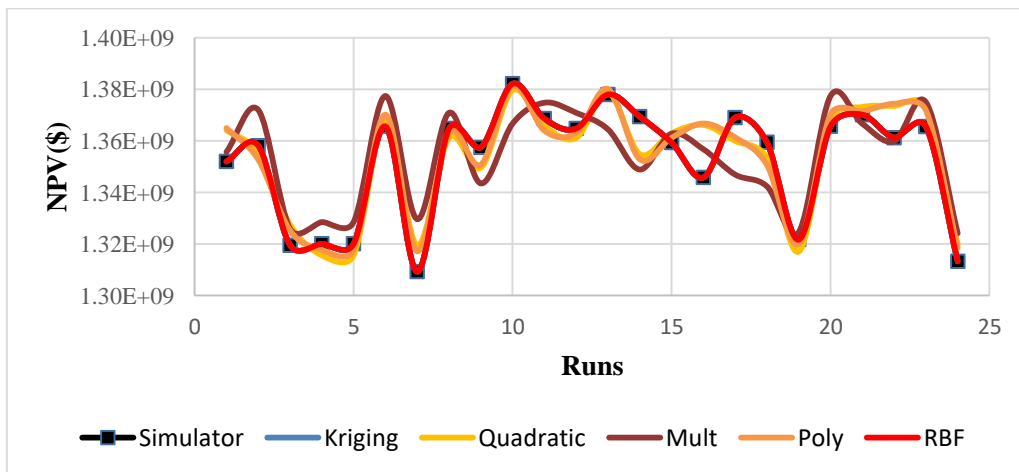


Figure 4.23a: Fitting results of surrogate models for Well 3 with selective initial points

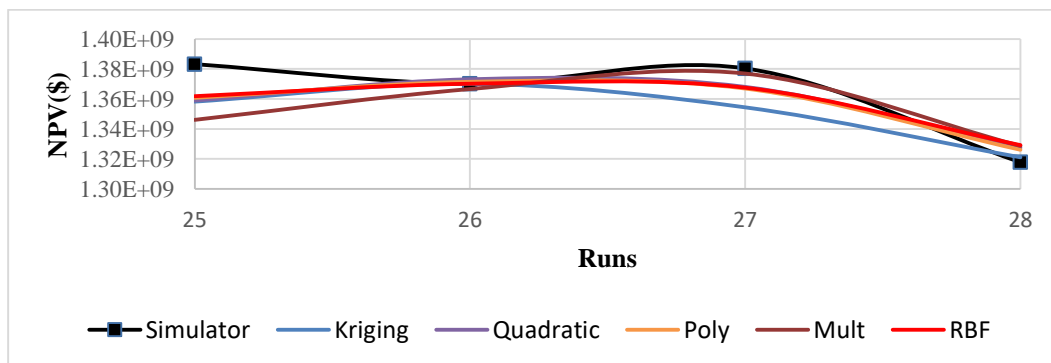


Figure 4.23b: Prediction results of surrogate models for Well 3 with selective initial points

Table 4.3: Summary of the performance indices of surrogate models for Well 3

Performance	Quadratic	Polynomial	Multiplicative	Kriging	RBF
AD	0.00	0.00	1284.90	1702338.15	814373.61
AAD	7341663.16	6861968.16	10833202.32	1936769.70	1629867.57
RMSE	9183951.31	9005346.48	13223467.59	6837599.56	5182970.82
E _{max}	1.51	1.56	1.55	0.25	0.87
AAPRE	0.54	0.51	0.80	0.14	0.12
SD	0.47	0.45	0.98	0.25	0.15
R ² _{fit}	0.92	0.92	0.81	0.99	0.99
R ² _{Pred}	0.89	0.90	0.78	0.88	0.90

4.3.4 Well 4

A method similar to those above was used. Five different surrogate models were considered. Similarly, Table 4.3 shows the results of the statistical analysis for each model. The fitting and prediction performance of each surrogate model was compared with that of the simulator, as shown in Figures 4.24a and 4.24b respectively. To compare the model, the predicted and simulator responses were plotted, as shown in Figures 4.24a and 4.24b. From the plot and performance indices, it was observed that both kriging and RBF have the best fitting tendencies with the multiplicative being the poorest as kriging is an exact data estimator because they tend to replicate the actual response rather than force fitting the expected model profile. Similarly, in the prediction graph (Figure 4.24b), it was observed that responses from the surrogate models matched the actual value accurately with appreciable error. The kriging-based and polynomial-based models were observed to perform the best but RBF and kriging outperformed both because of their fitting performance.

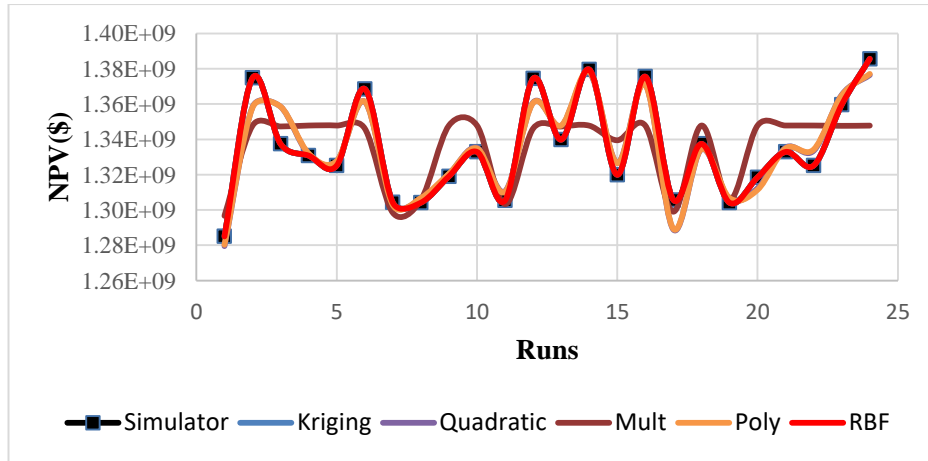


Figure 4.24a: Fitting results of surrogate models for Well 4 with selective initial points

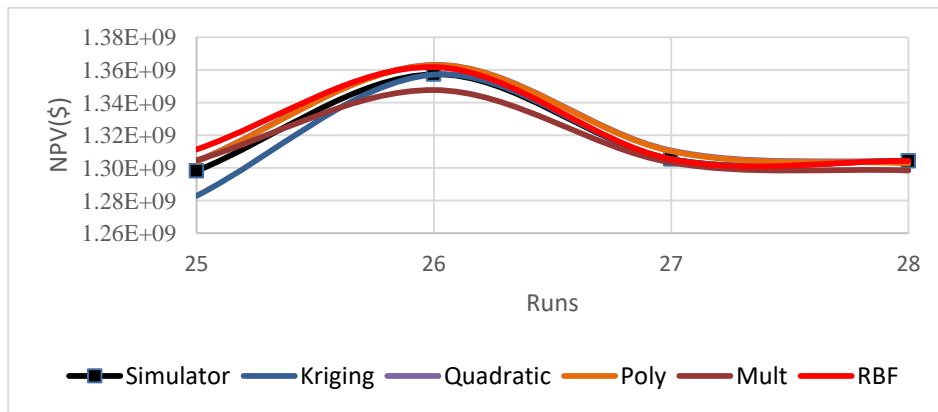


Figure 4.24b: Prediction results of surrogate models for Well 4 with selective initial points

Table 4.4: Summary of the performance indices of surrogate models for Well 4

Performance	Quadratic	Polynomial	Multiplicative	Kriging	RBF
AD	0.00	0.00	0.00	552907.54	-626670.11
AAD	6140056.58	6133884.29	15640656.24	552907.54	626670.11
RMSE	7980460.24	7968139.30	18786466.72	2886430.00	2618346.19
E _{max}	1.58	1.58	2.23	0.00	1.01
AAPRE	0.46	0.46	1.16	0.04	0.05
SD	0.37	0.37	2.00	0.05	0.04
R _{2_fit}	0.96	0.96	0.75	0.99	0.99
R _{2_Pred}	0.95	0.95	0.70	0.95	0.95

4.3.5 Well 5

Figures 4.25a and 4.25b show the fitting and prediction performance of each surrogate model compared with that of the simulator respectively. Also, the statistical analysis results for the quadratic, polynomial and multiplicative model constants, are as shown in Table 4.5. As shown in both figures, different colours depict the different proxy models' performances with black, blue, red, yellow, brown and green representing actual response, kriging, RBF, quadratic, multiplicative and polynomial respectively. To compare the model prediction with the actual data, the predicted and simulator responses were plotted, as shown in both graphs. From Figure 4.25 (a,b) and Table 4.5, it was observed that both kriging and RBF have the best fitting tendencies with the multiplicative being the poorest, as kriging and RBF are data-exact regenerators because they tend to replicate the actual response rather than force fit. In the prediction graph (Figure 4.25b), it was observed that responses from the surrogate models did not match the actual value accurately but showed appreciable error because of the noisy nature of the data characteristic of the dataset. The polynomial-based models were observed to perform better during prediction because of their ability to smooth out noise inherent in different data as data-exact predictors like kriging and RBF have been shown to underperform in noisy systems.

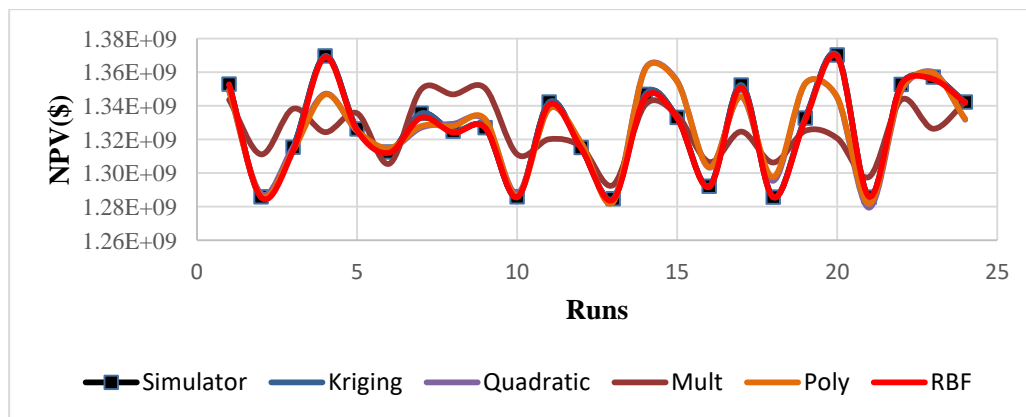


Figure 4.25a: Fitting results of surrogate models for Well 5 with selective initial points

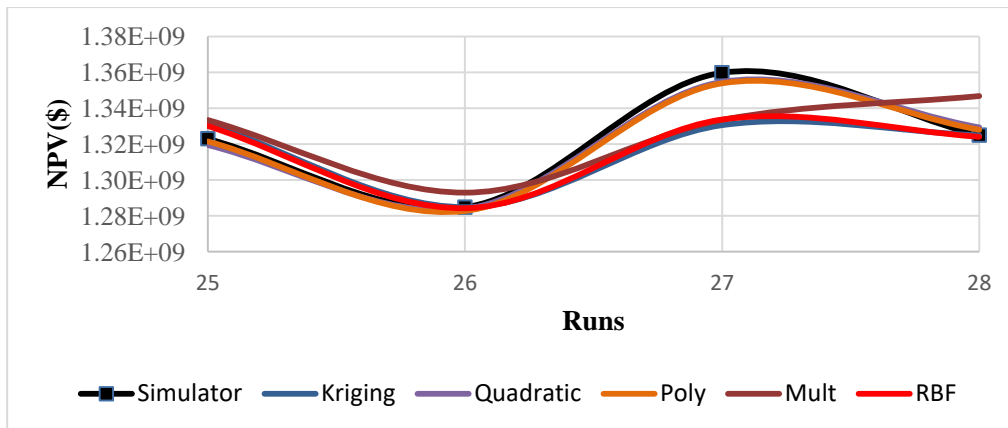


Figure 4.25b: Prediction results of surrogate models for Well 5 with selective initial points

Table 4.5: Summary of the performance indices of surrogate models for Well 5

Performance	Quadratic	Polynomial	Multiplicative	Kriging	RBF
AD	0.00	0.00	198.73	738889.19	1379439.31
AAD	7397192.65	7201179.25	17177299.85	1360088.71	1915917.11
RMSE	10226732.87	10167121.68	20980431.50	5750495.54	5203186.23
Emax	1.63	1.60	1.97	0.64	0.55
AAPRE	0.55	0.54	1.29	0.10	0.14
SD	0.60	0.59	2.54	0.19	0.15
R2_fit	0.93	0.93	0.64	0.99	0.96
R2_Pred	0.92	0.93	0.60	0.88	0.88

4.3.6 Well 6

Similarly, Table 4.6 depicts the model performance indices: quadratic, polynomial and multiplicative model constants. Figures 4.26a and 4.26b show the performance of fitting and prediction of each surrogate model compared to that of the respective simulator. In obtaining these models, a method similar to that used above was used. Five different surrogate models were considered in modelling this response. The regression coefficients of each model were obtained using MATLAB[®] and JMP. Different colours depict the different proxy models' performance with black, blue, red, yellow, brown and green representing Eclipse[®] 100 simulator output, kriging, RBF, quadratic, multiplicative and polynomial respectively. To compare the model prediction with the actual data, the predicted and simulator responses were plotted as shown in both graphs. From the graph, it was observed that both kriging and RBF

had the best fitting tendencies because of their lower estimation error and had the highest values of correlation coefficients, with the multiplicative being the poorest. In the prediction graph (Figure 4.26b), it was observed that responses from the surrogate models matched the actual value accurately with appreciable error. The RBF-based models were observed to replicate the trend of simulation predictions best but the quadratic model outperformed both because of its force-fitting nature.

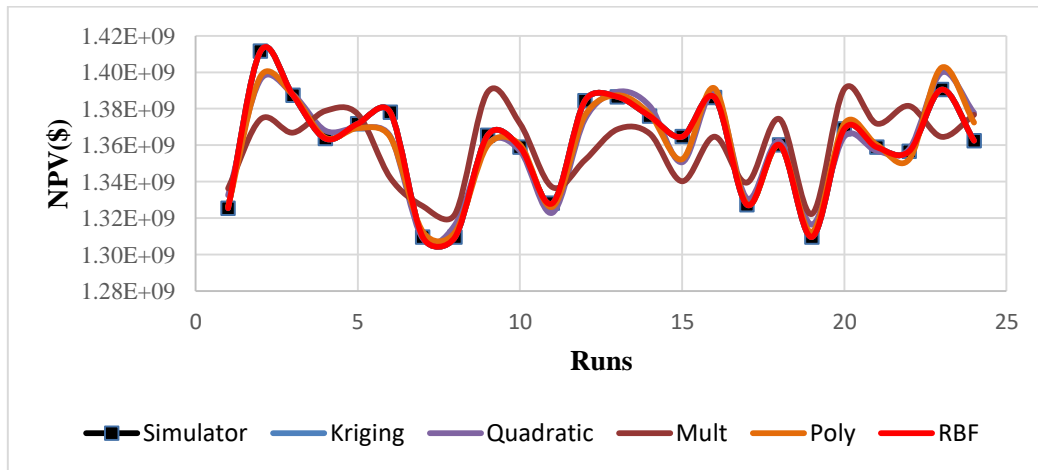


Figure 4.26a: Fitting results of surrogate models for Well 6 with selective initial points

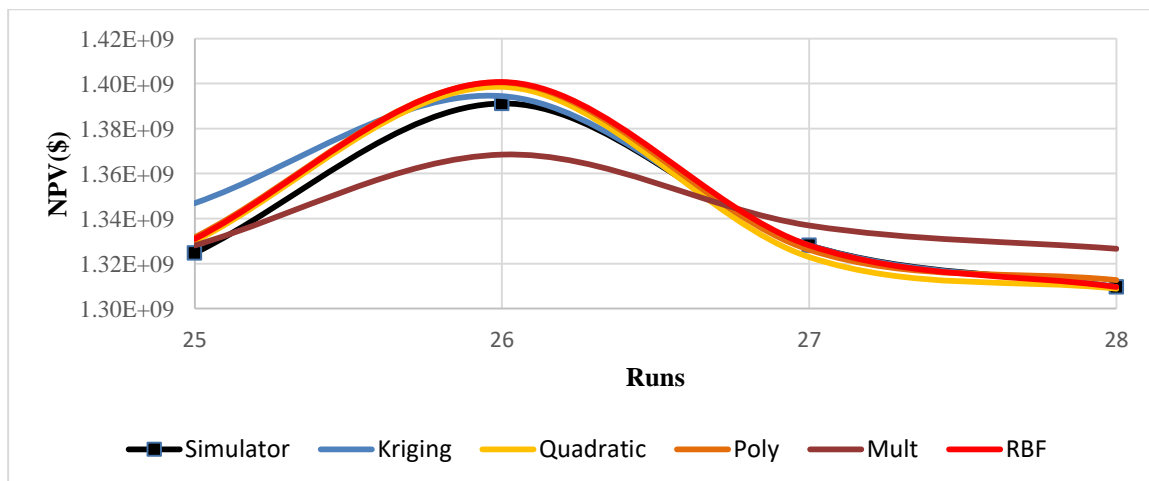


Figure 4.26b: Prediction results of surrogate models for Well 6 with selective initial points

Table 4.6: Summary of the performance indices of surrogate models for Well 6

Performance	Quadratic	Polynomial	Multiplicative	Kriging	RBF
AD	0.00	0.00	963.46	-908141.21	-563459.56
AAD	5736075.95	4592287.14	17747384.56	908141.21	563459.56

RMSE	7205829.71	6301800.64	19649618.77	4235276.36	2152340.28
Emax	1.12	0.87	1.83	1.67	0.68
AAPRE	0.42	0.34	1.30	0.07	0.04
SD	0.29	0.22	2.13	0.11	0.03
R2_fit	0.97	0.98	0.74	0.99	0.99
R2_Pred	0.96	0.97	0.73	0.93	0.96

4.3.7 Well 7

Five different surrogate models were also considered in this section. Similarly, Table 4.7 shows the results of the statistical analysis of each surrogate. The fitting and prediction performance of each surrogate model was also compared with that of the simulator as shown in Figures 4.27a and 4.27b. Black, blue, red, yellow, brown and green colours respectively depict Eclipse® 100 simulator output, kriging, RBF, quadratic, multiplicative and polynomial. From the plot and performance indices, it was observed that both kriging and RBF have the best fitting tendencies with the multiplicative being the poorest. In the prediction crossplot (Figure 4.27b), it was observed that responses from the surrogate models matched the actual value accurately with appreciable error with kriging and RBF having the lowest estimation error with highest values of correlation coefficients.

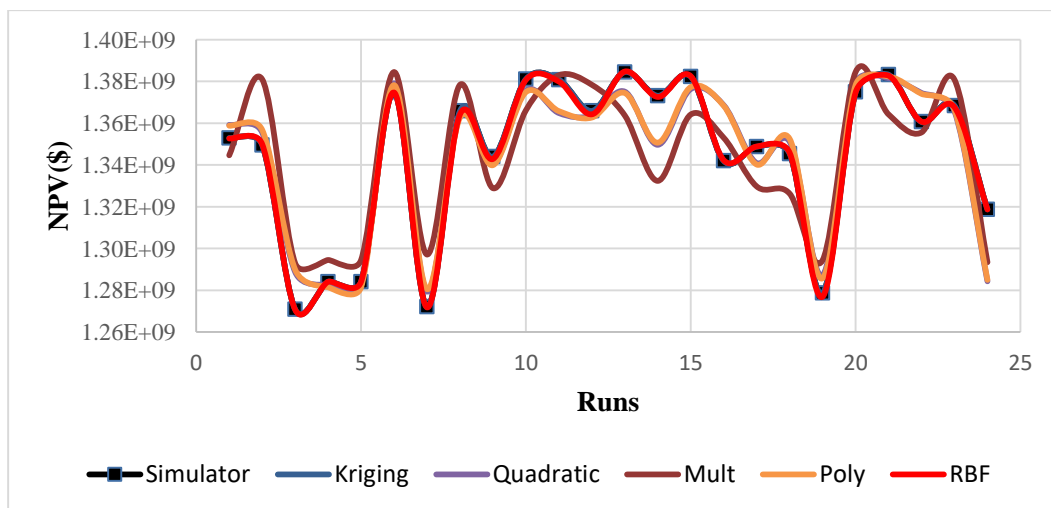


Figure 4.27a: Fitting results of surrogate models for Well 7 with selective initial points

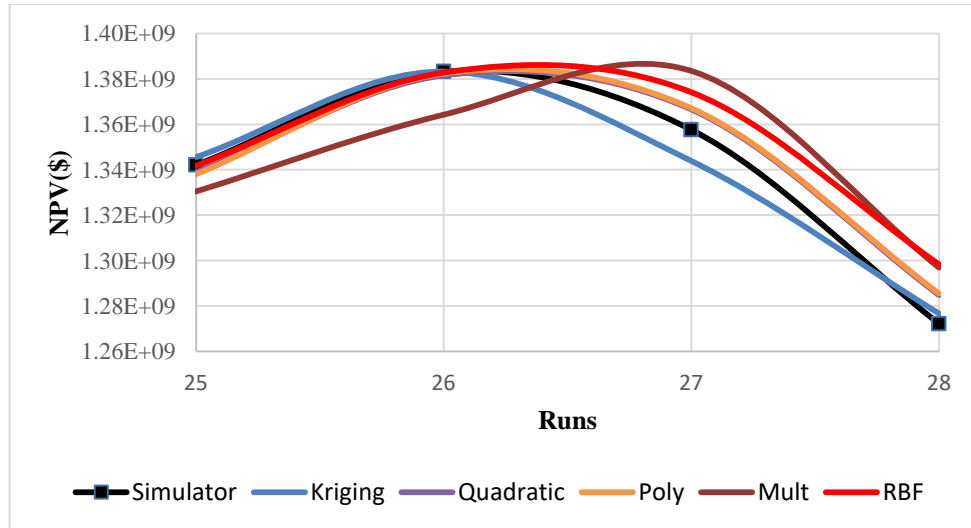


Figure 4.27b: Prediction results of surrogate models for Well 7 with selective initial points

Table 4.7: Summary of the performance indices of surrogate models for Well 7

Performance	Quadratic	Polynomial	Multiplicative	Kriging	RBF
AD	0.00	0.00	2232.98	206168.69	-1212982.44
AAD	8752043.36	8873152.51	16848527.81	773732.93	1974138.81
RMSE	11934479.26	11900853.98	18727997.74	2804748.17	5881141.05
Emax	1.99	1.97	2.33	0.35	2.05
AAPRE	0.65	0.66	1.26	0.06	0.15
SD	0.83	0.83	2.03	0.04	0.21
R2_fit	0.95	0.95	0.87	0.99	0.99
R2_Pred	0.93	0.94	0.85	0.97	0.90

4.3.8 Well 8

Figure 4.28a and 4.28b show the fitting and prediction performance of each surrogate model compared to that of the respective simulator respectively. In addition, the statistical analysis indices are shown in Table 4.8. As shown in both figures, different colours depict the different models' performance. From the plot and performance indices, it was observed that both kriging and RBF have the best fitting tendencies with the multiplicative being the poorest as kriging and RBF are data exact regenerators because they tend to replicate the actual response rather than force fit. In the prediction plot (Figure 4.28b), it was observed that responses from the surrogate models did not match the actual value accurately but had appreciable

error because of the noisy nature of the data characteristic of the dataset. The kriging- and polynomial-based approaches were observed to have performed best but the prior poor fitting performance of the latter makes kriging the better surrogate for the well being studied.

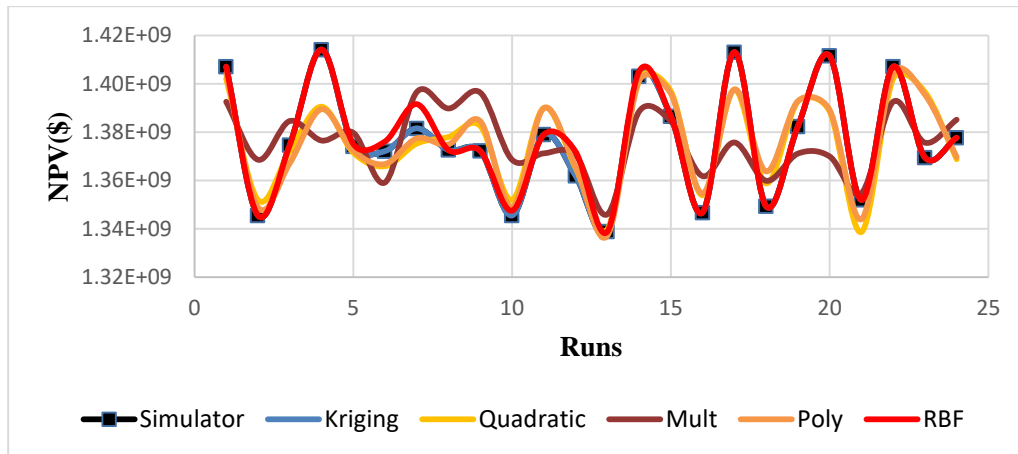


Figure 4.28a: Fitting results of surrogate models for Well 8 with selective initial points

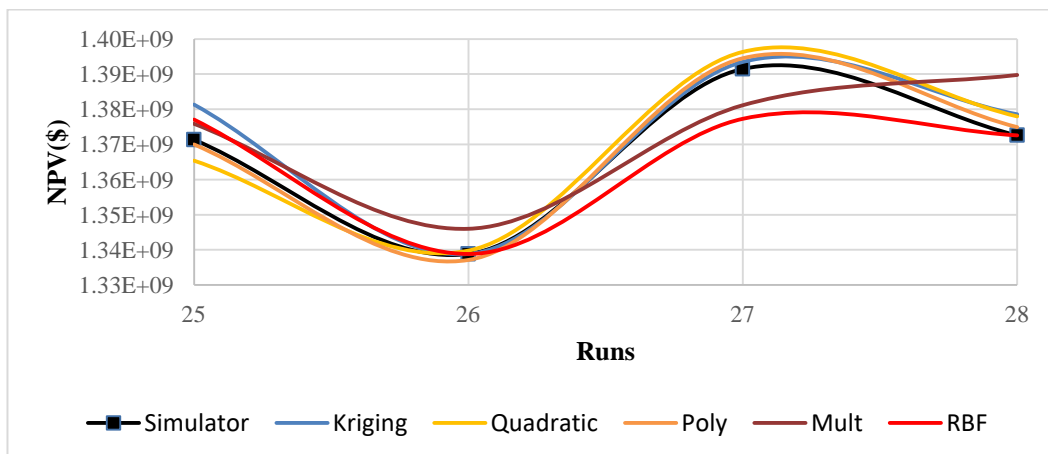


Figure 4.28b: Prediction results of surrogate models for Well 8 with selective initial points

Table 4.8: Summary of the performance indices of surrogate models for Well 8

Performance	Quadratic	Polynomial	Multiplicative	Kriging	RBF
AD	0.00	0.00	1019.52	-642857.14	-733981.04
AAD	8532859.62	7833269.16	14623075.31	642857.14	1747306.06
RMSE	10788480.13	10489188.82	17807102.05	2236067.98	4049616.72
E _{max}	1.98	1.90	1.76	0.73	0.73

AAPRE	0.62	0.57	1.06	0.05	0.13
SD	0.63	0.59	1.70	0.03	0.09
R2_fit	0.90	0.92	0.75	0.99	0.98
R2_Pred	0.90	0.91	0.73	0.98	0.85

4.3.9 Well 9

Similarly, Table 4.9 presents the error analysis of the quadratic, polynomial and multiplicative models. Figures 4.29a and 4.29b show the performance of fitting and the prediction of each surrogate model compared to that of the simulator. In obtaining these models, methods similar to the above were used. Five different surrogate models were also considered. The regression coefficients of each model were obtained using MATLAB[®] and JMP. Colours black, blue, red, yellow, brown and green represent simulator output, kriging, RBF, quadratic, multiplicative and polynomial respectively. The models were compared, as can be seen in both Figures 4.29a and 4.29b, and Table 4.9. A similar trend to other wells' surrogate models was observed, with both kriging and RBF approaches being the best while multiplicative was the poorest. In the prediction graph (Figure 4.29b), it was observed that the kriging response had the best prediction trend with appreciable error compared to others. The polynomial-based models were observed to replicate the trend of simulation predictions but were marred by prior poor fitting ability.

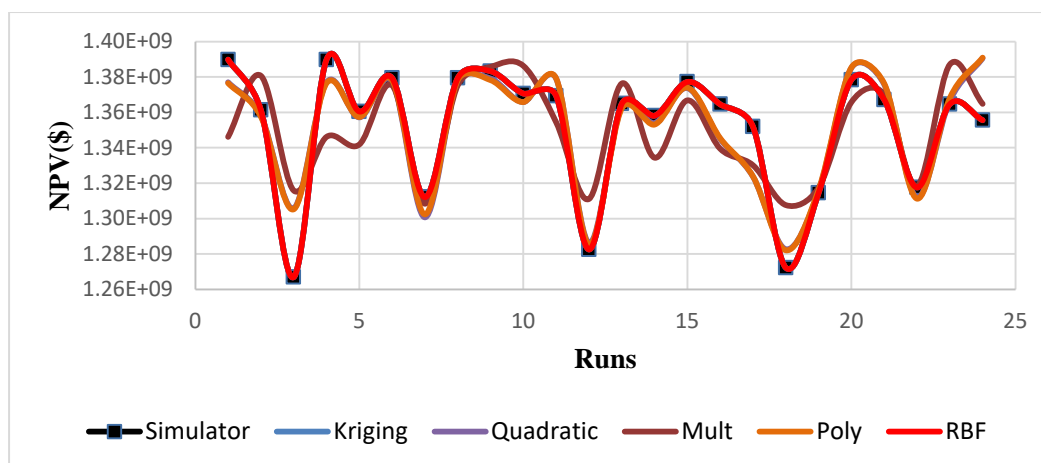


Figure 4.29a: Fitting results of surrogate models for Well 9 with selective initial points

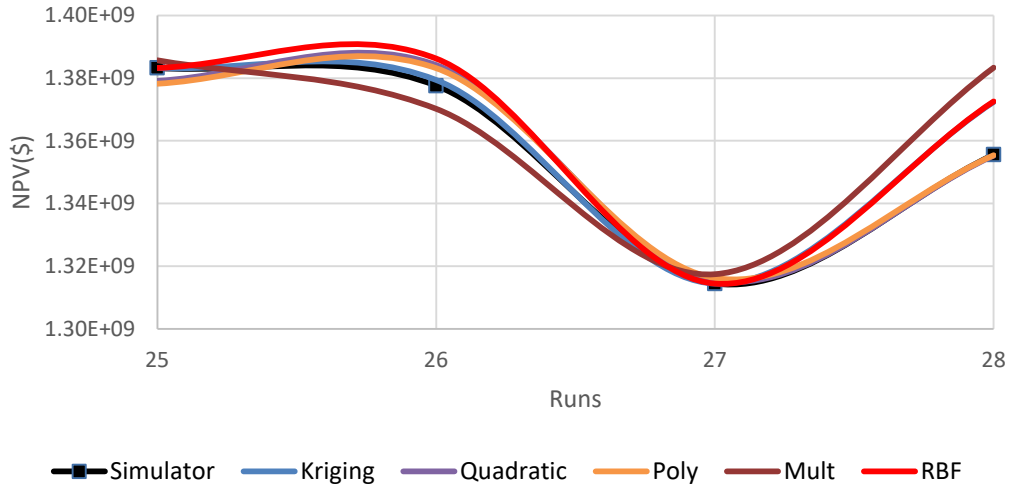


Figure 4.29b: Prediction results of surrogate models for Well 9 with selective initial points

Table 4.9: Summary of the performance indices of surrogate models for Well 9

Performance	Quadratic	Polynomial	Multiplicative	Kriging	RBF
AD	0.00	0.00	2283.87	-665682.01	-916146.33
AAD	8837698.59	8933753.66	16692781.87	665682.01	916146.34
RMSE	13235880.81	13215344.73	21569954.97	3197741.44	3604895.27
Emax	3.07	3.03	3.86	1.24	1.25
AAPRE	0.66	0.67	1.24	0.05	0.07
SD	1.03	1.03	2.70	0.06	0.07
R2_fit	0.93	0.93	0.79	0.99	0.98
R2_Pred	0.93	0.93	0.78	0.98	0.88

4.3.10 Well 10

The result of the error analysis and the regression coefficients of quadratic, polynomial and multiplicative model are shown in Table 4.10. Figures 4.30a and 4.30b show the extent of the fitting and prediction of the aforementioned surrogates. In obtaining these models, methods similar to those above were used. Five different surrogate models were also considered. The regression coefficients of each model were obtained using MATLAB[®] and JMP. Colours black, blue, red, yellow, brown and green represent simulator output, kriging, RBF, quadratic, multiplicative and polynomial respectively. The models were compared, as shown in both Figures 4.30a and 4.30b, and Table 4.9, and a similar trend to other wells' surrogate models

was observed; both the kriging and RBF approaches were the best while the multiplicative approach was the poorest. In the prediction graph (Figure 4.30b), it was observed that the kriging response had the best prediction trend with appreciable error, in other words, the least estimation error and highest values of correlation coefficients compared to others. The polynomial-based models were observed to replicate the trend of simulation predictions but were marred by prior poor fitting ability.

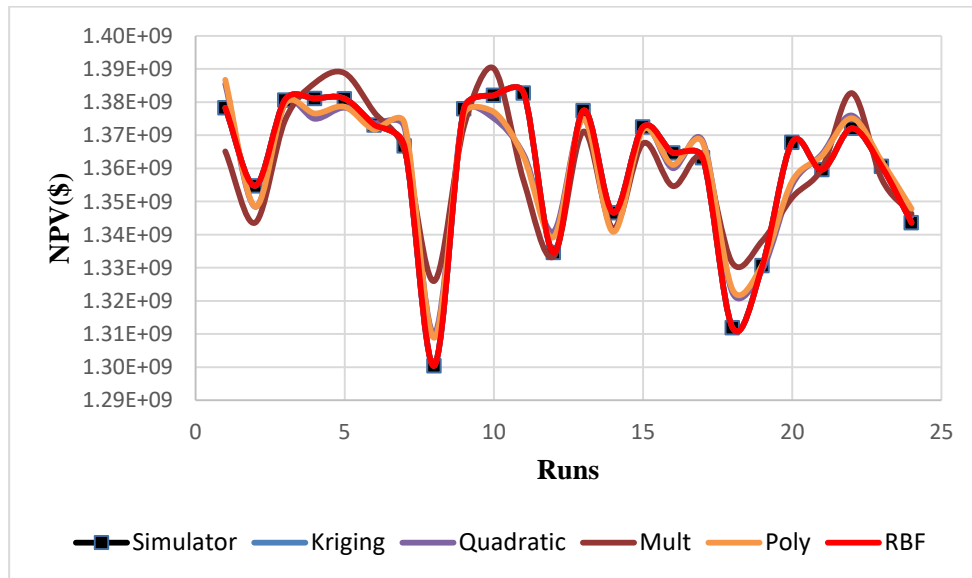


Figure 4.30a: Fitting results of surrogate models for Well 10 with selective initial points

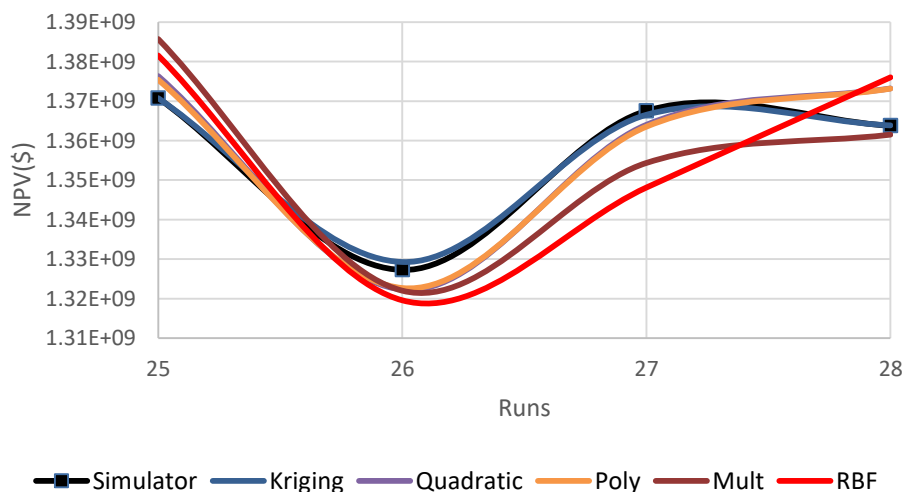


Figure 4.30b: Prediction results of surrogate models for Well 10 with selective initial points

Table 4.10: Summary of the performance indices of surrogate models for Well 10

Performance	Quadratic	Polynomial	Multiplicative	Kriging	RBF
AD	0.01	0.00	-186.67	131669.64	-219963.90
AAD	5695615.86	5639227.10	8569221.32	1002188.41	1220673.73
RMSE	7494688.73	7396738.65	10910440.29	3188626.99	3519185.12
E _{max}	1.48	1.42	1.97	0.90	1.07
AAPRE	0.42	0.42	0.63	0.07	0.09
SD	0.32	0.31	0.68	0.06	0.07
R ² _{fit}	0.91	0.92	0.75	0.99	0.99
R ² _{Pred}	0.90	0.90	0.72	0.93	0.90

4.3.11 Well 11

The results of the error analysis for the quadratic, polynomial and multiplicative model regression are shown in Table 4.11. Figures 4.31a and 4.31b show the performance of fitting and prediction of each surrogate model compared with that of the simulator respectively. In obtaining these models, a method similar to that of the above was used. From the fitting and statistical analysis results, it was observed that the kriging, RBF and quadratic approaches have the best fitting tendencies with the multiplicative being the poorest. In the prediction plot (Figure 4.31b), it was observed that responses from the surrogate models matched the actual value accurately with acceptable error. The kriging- and RBF-based models were observed to replicate the trend of simulation predictions but kriging outperformed all because of its ability to recreate the input-output distribution.

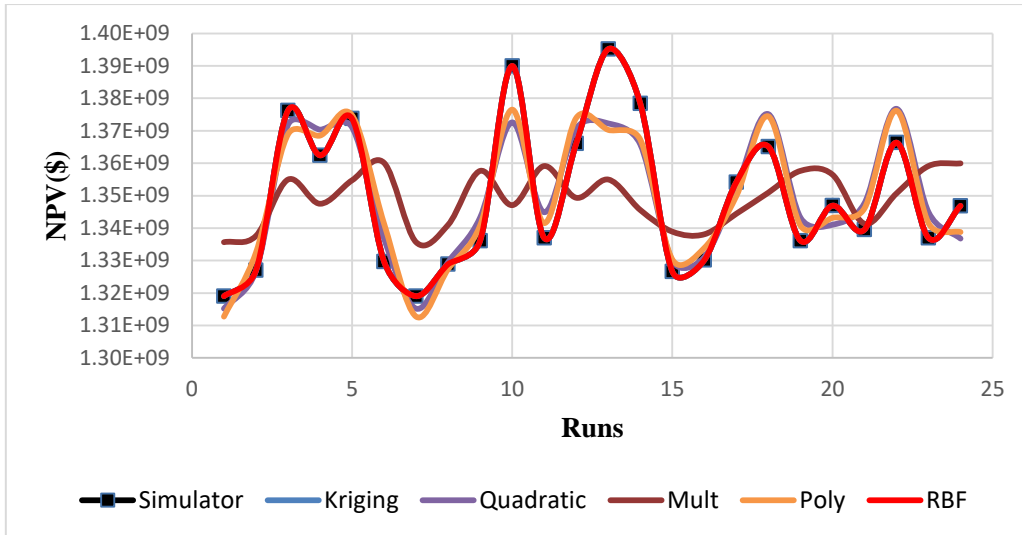


Figure 4.31a: Fitting results of surrogate models for Well 11 with selective initial points

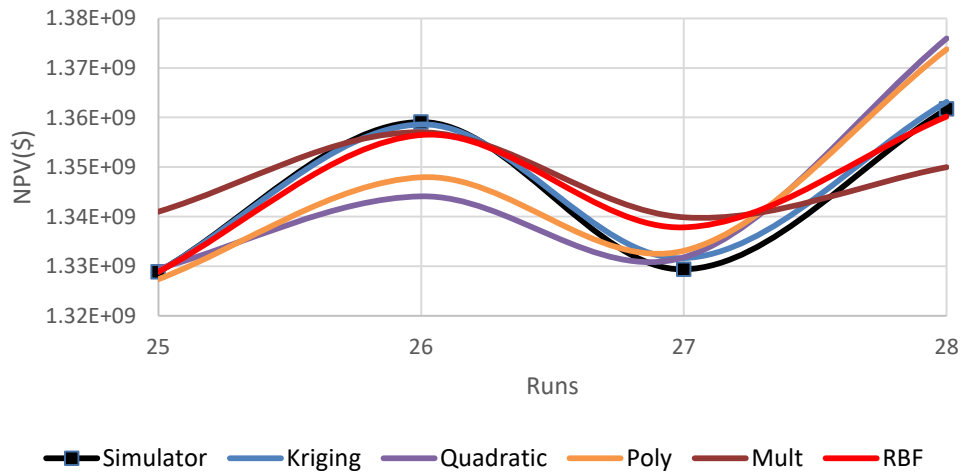


Figure 4.31b: Prediction results of surrogate models for Well 11 with selective initial points

Table 4.11: Summary of the performance indices of surrogate models for Well 11

Performance	Quadratic	Polynomial	Multiplicative	Kriging	RBF
AD	0.00	0.00	-214.15	115076.34	-155265.46
AAD	7183164.12	7120532.97	17226823.67	149526.34	450037.53
RMSE	8992831.33	8557934.85	19744458.79	514855.31	1700138.26
E _{max}	1.05	0.88	2.29	0.17	0.64
AAPRE	0.53	0.52	1.27	0.01	0.03
SD	0.45	0.41	2.18	0.00	0.02
R ² _{fit}	0.91	0.92	0.38	0.99	0.99
R ² _{Pred}	0.88	0.89	0.40	0.93	0.91

In this research work, it was observed that each surrogate model performed differently during the fitting and prediction phase as occasioned by the ability of each model to correctly mimic the noisy, nonlinearities distribution inherent in the process. The accuracy of each model is dependent on the extent of fit between the surrogate and simulation results and the ability to recreate the response distribution as the input varies. From all surrogates' estimation, it was observed that kriging and RBFs have the best fitting performance as this is dependent on the nature of kriging models, type of basis function and shape parameter used as there is no universal model for every study. Kriging and RBF are exact interpolation techniques because they require every data point in the n-dimensional input vector to be mapped onto the corresponding target output, therefore, both models perform poorly within a noisy dataset and are not mathematically computationally efficient. However, they perform excellently as a black box model due to their generalization and cost efficiency.

4.4 Optimization

In this section, optimization of the desired objective function, in other words, discounted net cash flow (NPV at 0% and 20%), was carried out. The objective function is to maximize the net present value of the investment as given by the selected surrogate model, namely, kriging and RBF models. The maximization was aimed at determining optimal placement of each horizontal well. Design variables

include the heel, length and direction of the horizontal well. In this optimization task, the number and location of wells were fixed as they had been optimized using the TPLHD approach, as earlier explained, and therefore could not be varied.

The optimization is a constrained integer-based genetic algorithm optimization technique as its parameter variation is bounded. Inequality constraint was used as shown in Equation 4.1. As it was the objective to perform a surrogate-based optimization problem, the results are given below. Based on the observation, as suggested by Figures 4.32 – 4.34, it was observed that using the approach as outlined will result in 2MMSTB and 8% incremental in cumulative oil production and investment cash flow respectively. The significant change in the two most important objective functions shows the successful nature of the whole process if implemented in well placement problems.

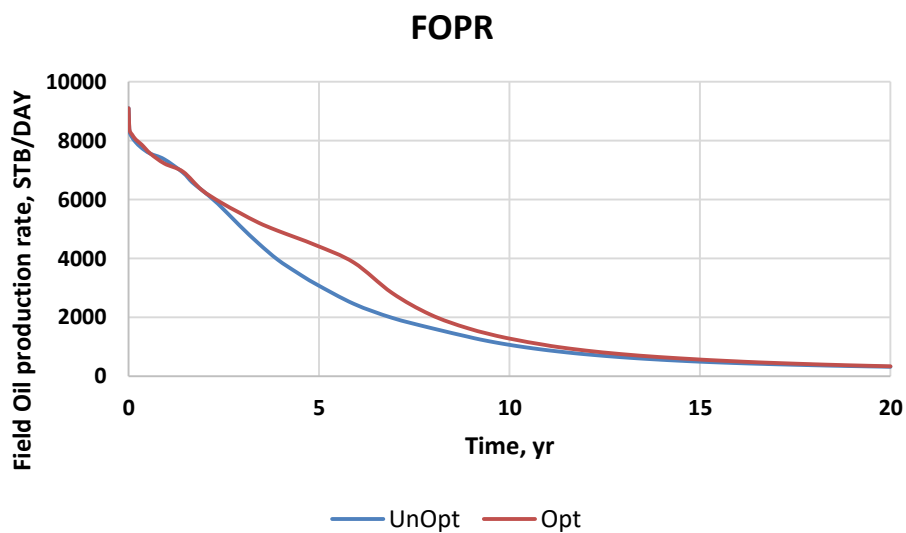


Figure 4.32: Field oil production rate of the two scenarios

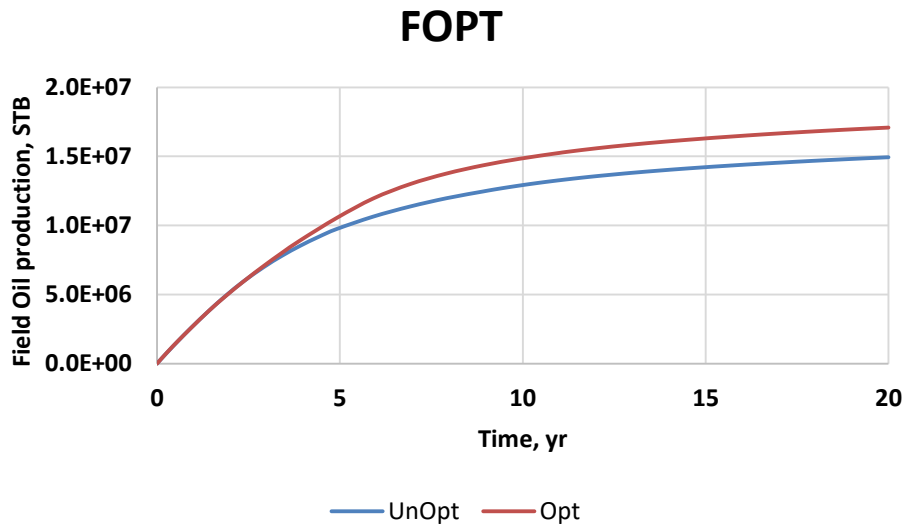


Figure 4.33: Field cumulative oil production of the two scenarios

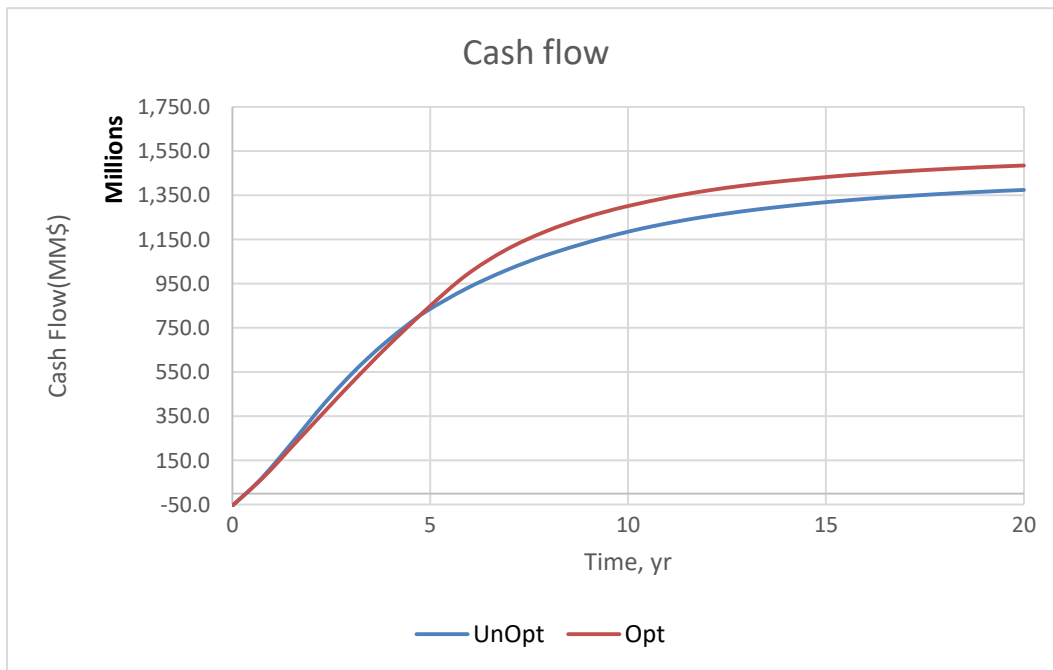


Figure 4.34: Comparison of investment cash flow of the two scenarios

CHAPTER FIVE: CONCLUSIONS AND RECOMMENDATIONS

5.1 Conclusions

In this study, an integrated framework was proposed to achieve this aim. The proposed model implemented a framework using numerical simulation software. The economic parameter, namely, net present value (NPV) was used as the desired optimizable objective function. From the results obtained it was shown that:

1. Space filling design is a useful tool in determining and optimizing the number and location of wells in a well placement optimization task and useful in obtaining initial points for a surrogate model as it accounts for the distance between selected points while ensuring balance between the sample locations.

2. Various surrogates exist but that a geometric-based model has the best prediction performance while polynomial-based models performed reasonably well because of their noise smoothing property. Polynomial-based models such as quadratic and polynomial are useful for the quick estimation of any desired function whereas geometric-based models should be used when near-accurate estimates are required. For the geometric model, radial basis function shows a better prospect than kriging but its performance hinges on the shape parameter and type of radial basis function but it underperforms with fewer datasets with noise.

3. The best surrogates obtained using the numerical tool are validated and optimized using genetic algorithm and it was observed that genetic algorithm as a popular optimization is an important tool in any optimization problem and NPV is a better indicator of investment return compared with cumulative oil production.

4. Approximately 8% return on investment was achieved.

5.2 Recommendations

The following set of recommendations is suggested for future studies:

- a. The complete automation of the methodology as outlined is recommended for future study.
- b. The validation of the framework using real life reservoir data and assessment of associated uncertainty.

REFERENCES

- Afshari S., Pishvaie M. R. & Aminshahidy B. (2013). Well Placement Optimization Using a Particle Swarm Optimization Algorithm, a Novel Approach. *Pet. Sci. Tech.* 32(2). pp. 170-179.
- Askari Firoozjaee, R. & Khomehchi, E. (2015). A novel approach to assist history matching using artificial intelligence. *J. Chem. Eng. Comm* 202 (4), 513-514.
- Awotunde A. A. (2014). On The Joint Optimization of Well Placement and Control. *Society of Petroleum Engineers (SPE)*. <https://doi.org/10.2118/172206-MS>.
- Babu, G. S. & Suresh, S. (2015). Sequential projection-based metacognitive learning in a radial basis function network for classification problems. *IEEE T NEUR NET LEAR*, vol. 24, no. 2, pp. 194–206.
- Bangerth W., Klie H., Wheeler M., Stoffa P., Sen M. (2006). On optimization algorithm for the reservoir oil well placement problem. *Comput. Geosci.* vol.10 pp. 303-319
- Beckner B. & Song X. (1995). Field development planning using simulated annealing – optimal economic well scheduling and placement. *Society of Petroleum Engineers (SPE)*. <https://doi.org/10.2118/30650-MS>
- Bittencourt, A. & Horne, R. (1997). Reservoir development and design optimization. *Society of Petroleum Engineers (SPE)*. <https://doi.org/10.2118/38895-MS>
- Chen H., Feng Q., Zhang X., Wang S., Zhou W. & Geng Y. (2017). Well placement optimization using an analytical formula-based objective function and cat swarm optimization algorithm. *J. Pet. Sci. Eng.* 157. Pp. 1067-1083.
- Ciaurri D. E., Mukerji T. & Durlinsky L. (2011). Derivative-Free Optimization for Oil Field Operations. *Computational Optimization and Applications in Engineering and Industry. Springer-Verlag Berlin Heidelberg.* vol 359 Pp. 19-55
- Couckuyt, I., Koziel S., & Dhaene, T., (2013). Surrogate modeling of microwave structures using kriging, co-kriging, and space mapping," *Int J Numer Model El.*, vol. 26, no. 1, pp. 64–73.
- Craft B. C., Hawkins M. & Terry R. E. (1959). Applied Petroleum Reservoir Engineering. 2nd ed. *Pearson*, London, UK.
- Davis, L. (1991). Handbook of Genetic Algorithms. *Van Nostrand Reinhold*, New York, NY.
- Ebadat A. & Karimaghvae P. (2012). Genetic Algorithm Assisted Fuzzy Iterative Learning Optimizer for Automatic Optimization of Oil well Placement under Production Constraints. *IFAC Proceedings* vol. 45:25 pp 223-228
- Eberhardt, R. C. & Kennedy, J. (1995). A new optimizer using particle swarm theory. In: *Proceedings of the 6th International Symposium on Micromachine and Human Science*, pp. 39–43.
- Ebrahimi, A. & Khomehchi, E. (2015). A robust model for computing pressure drop in vertical multiphase flow, *J. Nat. Gas Sci. Eng.*, 26: 1306-1316.
- Engelbrecht, A. P. (2005). Fundamentals of Computational Swarm Intelligence. *Wiley*, West Sussex, England.
- Fang, K. T., Lin, D., Winker, P., & Zhang, Y. (2000). Uniform design: Theory and application. *Technometrics*, vol. 42, no. 3, pp. 237-248.
- Giunta, A. A., Wojtkiewicz S, & Eldred, M. S. (2001). Overview of Modern Design of Experiments Methods for Computational Simulations. *AIAA paper* 2003-649.
- Goldberg D.E. Computer Aided Gas Pipeline Operation Using Genetic Algorithms and Rule Learning (1983). Ph.D. Dissertation. University of Michigan, Ann Arbor, Michigan.

- Guyaguler, B. (2003). Optimization of Well Placement and Assessment of Uncertainty. Ph.D. Thesis, Stanford University, Stanford, CA.
- Guyaguler B. & Horne N. (2001). Uncertainty Assessment of Well Placement Optimization. *SPE Annual Technical Conference and Exhibition*, 30 September-3 October, New Orleans, Louisiana. <https://doi.org/10.2118/71625-MS>
- Guerreiro J.N.C, Barbosa H., Garcia E., Loula A. & Malta S. (1998). Identification of reservoir heterogeneities using tracer breakthrough profiles and genetic algorithms. *SPE Res. Eval. Eng.* vol. 1(03). Pp. 218-223 <https://doi.org/10.2118/39066-PA>
- Han, Z. H., & Zhang K. S. (2012). Surrogate-based optimization, real-world applications of genetic algorithms. *IntechOpen*. <https://doi.org/10.5772/36125>
- Hosseini S. & Al Khaled A. (2014). A survey on the imperialist competitive algorithm metaheuristic: implementation in engineering domain and directions for future research. *Appl. Soft Comput.*, vol 24, pp. 1078-1094
- Jin, R., Chen, W., & Simpson, T. W. (2000). Comparative studies of Metamodeling techniques under multiple modeling criteria. *8th AIAA/NASA/USAF/ISSMO Symposium on Multi-Disciplinary Analysis and Optimization*, Long Beach, CA.
- Johnson, V. M. & Rogers, L. L. (2001). Applying soft computing methods to improve the computational tractability of a subsurface simulation-optimization problem. *J. Pet. Sci. Eng.*, 29, 153-175.
- Kennedy, J. & Eberhardt, R.C. (1995). Particle swarm optimization. *Proceedings of the IEEE International Joint Conference on Neural Networks, Piscataway*. pp. 1942–1947.
- Kitayama, K., Srirat, J., & Arakawa, M. (2013). Sequential approximate multi-objective optimization using radial basis function network. *Struct Multidiscip Optim*, vol. 48, no. 3, pp. 501–515.
- Lyons J. & Nasrabadi H. (2013). Well placement optimization under time-dependent uncertainty using an ensemble Kalman filter and a genetic algorithm. *J. Pet. Sci. Eng.* vol. 109 pp. 70-79
- Mohammadi, H., Seifi, A., & Foroud, T. (2012). A robust kriging model for predicting accumulative outflow from a mature reservoir considering a new horizontal well. *J. Pet. Sci. Eng.* vol. 82-83, 113-119. <https://doi.org/10.1016/j.petrol.2012.01.00>
- Montes G., Bartolome P., and Udais A. (2001). The Use of Genetic Algorithm in Well Placement Optimization. *Society of Petroleum Engineers (SPE)*. <https://doi.org/10.2118/69439-MS>
- Moravvej F. M. (2008). IMPROVING GENETIC ALGORITHMS FOR OPTIMUM WELL PLACEMENT. MSc. Thesis. Stanford University.
- Naderi M. & Khomehchi E. (2017). Well placement optimization using metaheuristic bat algorithm. *J. Pet. Sci. Eng.* vol.150, 348-354.
- Onwunalu, J. E. (2010). Optimization of Field Development Using Particle Swarm Optimization and New Well Pattern Descriptions. Ph.D. Thesis, Stanford University, Stanford, CA.
- Pan G., Ye P. & Wang P. (2014). A Novel Latin Hypercube Algorithm via Translational Propagation, *The Scientific World Journal*. vol 2014 pp 1-15. <https://doi.org/10.1155/2014/163949>
- Poli, R., Kennedy, J., & Blackwell, T. (2007). Particle swarm optimization. *Swarm Intelligence*. 1(1):33–57, 2007.

- Rasouli H., Rashidi F., Karimi B. & Khamehchi E. (2015). A surrogate integrated production modeling approach to long-term gas-lift allocation optimization *J. Chem. Eng. Commun.*, 202 (5). pp. 647-654
- Reed R.D. & Marks R.J. (1999). Neural Smithing: Supervised Learning in Feedforward Artificial Neural Networks. *The MIT Press, Cambridge*.
- Rwechungura, R. W., Dadashpour, M., & Kleppe J. (2011). Application of Particle Swarm Optimization for Parameter Estimation Integrating Production and Time Lapse Seismic Data. *SPE Offshore Europe Oil and Gas Conference and Exhibition, 6-8 September, Aberdeen, UK*. <https://doi.org/10.2118/146199-MS>
- Sacks, J. W., Welch, J., Mitchell, T. J., & Wynn, H. P. (1989). Design and analysis of computer experiments. *J. Stat. Sci.* 4, 409–435.
- Salmachi, A., Sayyafzadeh, M., & Haghghi, M. (2013). Infill well placement optimization in coal bed methanereservoirs using genetic algorithm. *Fuel*. 111, 248-258.
- Sayyafzadeh M., Haghghi M., Bolouri K. & Arjomand E. (2012). Reservoir characterisation using artificial bee colony optimisation. *APPEA*. 52(1), 115-128. <https://doi.org/10.1071/AJ11009>
- Simpson, T. W., Mauery, T. M., Korte, J. J., & Mistree, F. (1998). Comparison of response surface and Kriging models for multidisciplinary design optimization. *7th AIAA/USAF/NASA/ISSMO Symposium on Multidisciplinary Analysis & Optimization*, St. Louis, MI, AIAA-98-4755.
- Viana F., Venter G. & Balabanov V. (2009). An algorithm for fast optimal Latin hypercube design of experiments. *Int J Numer Methods Eng.* 82(02). pp. 135-156.
- Vu, K.K., D'Ambrosio, C., Hamadi, Y. and Liberti, L. (2017), Surrogate-based methods for black-box optimization. *Intl. Trans. in Op. Res.*, 24: 393-424. doi:10.1111/itor.12292
- Vukovic, N. & Miljkovic, Z. (2013). A growing and pruning sequential learning algorithm of hyper basis function neural network for function approximation. *Neural Networks*, vol. 46, pp. 210–226.
- Wang, M. & Zheng, C., (1997). Optimal remedial policy selection under general conditions. *Ground Water* 35(5), 757-764.
- Yao, W., Chen, X. Q., Huang, Y. Y., & Van Tooren, M., (2014). A surrogate-based optimization method with RBF neural network enhanced by linear interpolation and hybrid infill strategy. *Optimization Methods & Software*, vol. 29, no. 2, pp. 406–429.
- Yeten B., Durllofsky L. & Aziz K. Optimization of nonconventional well type, location, and trajectory. *SPE J.*, 8 (3). [ps://doi.org/10.2118/86880-PA](https://doi.org/10.2118/86880-PA)
- Yunfeng Xu, Ping Fan, Ling Yuan (2013), A Simple and Efficient Artificial Bee Colony. *Math. Probl. Eng.* vol. 2013. [doi:10.1155/2013/526315](https://doi.org/10.1155/2013/526315)